Central Role of Muc5ac Expression in Mucous Metaplasia and Its Regulation by Conserved 5′ Elements

Hays W. J. Young, Olatunji W. Williams, Divay Chandra, Lindsey K. Bellinghausen, Guillermina Pérez, Alberto Suárez, Michael J. Tuvim, Michelle G. Roy, Samantha N. Alexander, Seyed J. Moghaddam, Roberto Adachi, Michael R. Blackburn, Burton F. Dickey, and Christopher M. Evans

Department of Pulmonary Medicine, The University of Texas M. D. Anderson Cancer Center; Departments of Pediatric Medicine and Internal Medicine, Baylor College of Medicine; Institute of Biosciences and Technology, Texas A&M University System Houston Health Science Center; Department of Biochemistry and Molecular Biology, University of Texas Health Sciences Center, Houston, Texas; and Instituto Tecnológico y de Estudios Superiores de Monterrey, Monterrey, Nuevo León, México

Mucus hypersecretion contributes to morbidity and mortality in many obstructive lung diseases. Gel-forming mucins are the chief glycoprotein components of airway mucus, and elevated expression of these during mucous metaplasia precedes the hypersecretory phenotype. Five orthologous genes (MUC2, MUC5AC, MUC5B, MUC6, and MUC19) encode the mammalian gel-forming mucin family, and several have been implicated in asthma, cystic fibrosis, and chronic obstructive pulmonary disease pathologies. However, in the absence of a comprehensive analysis, their relative contributions remain unclear. Here, we assess the expression of the entire gel-forming mucin gene family in allergic mouse airways and show that Muc5ac is the predominant gel-forming mucin induced. We previously showed that the induction of mucous metaplasia in ovalbumin-sensitized and -challenged mouse lungs occurs within bronchial Clara cells. The temporal induction and localization of Muc5ac transcripts correlate with the induced expression and localization of mucin glycoproteins in bronchial airways. To better understand the tight regulation of Muc5ac expression, we analyzed all available 5′-flanking sequences of mammalian MUC5AC orthologs and identified evolutionarily conserved regions within domains proximal to the mRNA coding region. Analysis of luciferase reporter gene activity in a mouse transformed Clara cell line demonstrates that this region possesses strong promoter activity and harbors multiple conserved transcription factor–binding motifs. In particular, SMAD4 and HIF-1α bind to the promoter, and mutation of their recognition motifs abolishes promoter function. In conclusion, Muc5ac expression is the central event in antigen-induced mucous metaplasia, and phylogenetically conserved 5′ noncoding domains control its regulation.

Keywords: mucin; metaplasia; airway; lung; epithelium

CLINICAL RELEVANCE

Mucus hypersecretion is associated with asthma and chronic obstructive pulmonary disease. MUC5AC is the most abundant gel-forming mucin present at the airway surface. Determining its expression and regulation in mice will allow us to identify its function and potentially useful and novel targets.

In the lungs, the conducting airways are lined by ciliated and nonciliated epithelial cells residing beneath a multiphase mucus film that has a superficial periciliary layer and an overlaying gel layer. Airway mucus is comprised of water, ions, polypeptides, cells, and cellular debris that are contained within a viscoelastic glycoprotein-rich gel (1). Functionally, airway mucus prevents desiccation of the underlying epithelium and traps inhaled particles and pathogens, allowing for their elimination by mucociliary clearance. Under healthy conditions, the steady-state regulation of the height and osmolarity of the periciliary layer and the thickness and composition of the gel layer allows for efficient mucociliary clearance. However, in obstructive lung diseases such as asthma, cystic fibrosis (CF), constrictive bronchiolitis, and chronic obstructive pulmonary disease (COPD), as well as in animal models of these diseases, mucus hypersecretion results in worsening of morbidity and mortality (for reviews, see Refs. 2 and 3). The hallmark of this mucous phenotype is elevated mucin production by surface epithelial cells, especially within the small (< 2 mm diameter) airways, by a process termed mucous (or goblet cell) metaplasia. In humans and in antigen-challenged mice, mucin production occurs via the induction of mucin gene expression within Clara cells (4, 5). In mice, this process occurs via activation of type 2 helper T-lymphocyte (Th2) (6) and epidermal growth factor (EGF) (7) signal transduction pathways.

Mucins are very high molecular weight glycoproteins that can either be membrane associated or secreted and released into the extracellular space. Membrane mucins are ubiquitously expressed by epithelia in respiratory mucosae, and they participate in cell adhesion and glycocalyx generation; they may also be secreted into the mucus layer as the result of shearing or the synthesis of splice variants lacking transmembrane domains (8, 9). Secreted mucins are expressed by nonciliated epithelial cells in the respiratory epithelium, and they are stored in intracellular secretory granules until stimulated for release by regulated exocytosis. A subset of secreted mucins, the gel-forming mucins, have large heavily O-glycosylated apoprotein cores (> 300 kD) as well as N- and C-terminal cysteine-rich von Willebrand Factor–like domains that participate in disulfide bond-mediated oligimerization. Once secreted, gel-forming mucins create very large (1 to > 10 MegaDalton) viscoelastic macromolecular complexes (10).

(*Received in original form December 15, 2005 and in final form March 27, 2007*)

This work was funded by NIH Grants R01HL72984 (B.F.D.), R01AI43572 (M.R.B.), F32HL082446 (H.W.J.Y), and by American Heart Association, Texas Affiliate Beginning Grant-in-Aid 0506030Y, Cystic Fibrosis Foundation Pilot and Feasibility Award 061O, and American Lung Association Biomedical Reseeach Grant RG-22720-N (C.M.E.). Research in animals was also supported by the M. D. Anderson Cancer Center Support Core Grant NIH/NCI CA16672.

Correspondence and requests for reprints should be addressed to Christopher M. Evans, Ph.D., Assistant Professor, Department of Pulmonary Medicine, M. D. Anderson Cancer Center, Institute of Biosciences and Technology, 2121 West Holcombe Boulevard, Room 703A, Houston, TX 77030. E-mail: cevans@mdanderson.org

This article has an online supplement, which is accessible from this issue's table of contents at www.atsjournals.org

Am J Respir Cell Mol Biol Vol 37. pp 273–290, 2007
Originally Published in Press as DOI: 10.1165/rcmb.2005-0460OC on April 26, 2007
Internet address: www.atsjournals.org

Five orthologous human and mouse genes encode the gel-forming mucins. Four of these (MUCs 2, 5AC, 5B, and 6) are present in tandem as a conserved cluster on human chromosome 11p15 and on the syntenic mouse chromosome 7 F5 (11). The fifth gel-forming mucin gene, MUC19, is present on chromosome 12q12 in humans and 15 E3 in mice (12, 13). MUC5AC and MUC5B have been implicated as markers of goblet cell metaplasia in lung pathologies based upon expression studies in humans, in animal models, and in cell cultures (14–19). Recently, some studies have also suggested involvement by MUC2 (20–22) and MUC19 (12). However, none of these studies tested the relative expression of the full set of gel-forming mucins in a comprehensive manner. Thus, ambiguity remains regarding the expression of these key molecules in lung physiology and pathophysiology.

Here, we quantitatively analyze the expression of the entire gel-forming mucin family in a mouse model of allergic airway inflammation. We show that Muc5ac is selectively induced in the metaplastic airways of antigen-challenged mice. We also show that specific motifs within evolutionarily conserved regions (ECRs) in the 5′ flanking region of mouse Muc5ac determine its transcriptional activity in a Clara cell line *in vitro*. Together, these studies provide a comprehensive analysis of the mucin gene expression patterns that are central to the development of airway goblet cell metaplasia *in vivo*, and they identify regions within the Muc5ac promoter that potently regulate its transcriptional activation.

MATERIALS AND METHODS

Animal Sensitization and Challenge

Female, specific pathogen–free, 6- to 8-wk-old C57BL/6J mice were purchased from Harlan (Indianapolis, IN). SV40 Large T Antigen transgenic mice were generated previously (23). Mice were housed in accordance with the Institutional Animal Care and Use Committee of the M. D. Anderson Cancer Center. Wild-type mice were sensitized to ovalbumin (20 μg ovalbumin Grade V, 2.25 mg alum in saline, pH 7.4; Sigma, St. Louis, MO) administered by intraperitoneal injection) four times, weekly. Sensitized mice were exposed for 30 min to an aerosol of either 0.9% (wt/vol) saline or 2.5% (wt/vol) ovalbumin in 0.9% saline, which were both supplemented with 0.02% (vol/vol) antifoam A silicon polymer (Sigma), via an AeroMist CA-209 compressed gas nebulizer (CIS-US, Inc., Bedford, MA) in the presence of room air supplemented with 5% CO_2, as described previously (5). At 6 h and 1, 2, 3, and 7 d after antigen challenge, animals were anesthetized by intraperitoneal injection of a mixture of ketamine, xylazine, and acepromazine. Under deep anesthesia, animals were tracheostomized using a 20-gauge blunt tip cannula and killed by exsanguination via the abdominal aorta. We have characterized the development and resolution of mucous metaplasia in this animal model extensively in the past (5), and the time points chosen for these experiments coincide with the development (6 h and 1–2 d) and peak (3–7 d) of mucin production following a single antigen aerosol challenge.

RNA Isolation and RT-PCR

Before isolation of RNA, tissues were removed from killed mice, immediately washed in diethylcarbamate (DEPC)-treated PBS, and snap-frozen in liquid N_2. For total RNA extraction, tissues were thawed in TRIZOL reagent (Invitrogen-Life Technologies, Carlsbad, CA), minced with a stainless steel razor blade, and passed three times through a 20-G needle. RNA was quantified by ultraviolet absorbance at 260 nm using a Nanodrop ND-1000 Spectrophotometer (NanoDrop Technologies, Wilmington, DE). Ten micrograms of total RNA was reverse transcribed (Superscript III; Invitrogen-Life Technologies) using random 9-mers (New England Biolabs, Beverly, MA) as complementary DNA (cDNA) primers in a 40-μl reaction. Primer pairs and Genbank sequences used to generate RT-PCR products are shown in Table 1. For nonquantitative RT-PCR analysis of mucin transcript expression, reverse-transcribed cDNA corresponding to 1 μg of starting RNA from the RT mixture was amplified in the appropriate primer extension mixture 33 times (94°C heating, 60°C annealing, 72° extension). For quantitative PCR, real-time PCR primers and 5′-FAM/3′-BHQ labeled Taqman probes were generated for Muc2, Muc5ac, Muc5b, and Muc19 using ABI Systems analysis software (Applied Biosystems, Foster City, CA; *see* Table 1). Quantitative PCR was then performed on cDNA corresponding to 100 ng of starting RNA from the RT mixture using Taqman probe assays on an ABI PRISM 7000 Sequence Detection System (Applied Biosystems). Generation of a standard curve was performed by PCR amplification of dilutions (0.001–100.0 pg) of synthetic single stranded oligonucleotide templates for each transcript. Final data were normalized to 18S transcripts per sample and expressed as the absolute numbers of molecules of query transcript per absolute numbers of molecules of 18S rRNA.

Histologic Preparation

Lungs were perfused with saline via the right cardiac ventricle to clear blood from the pulmonary tissues. Fixative (4% paraformaldehyde in DEPC-treated 0.1 M phosphate buffer, pH 7.0) was infused intratracheally at 10–15 cm pressure. The lungs were fixed *in situ* for 30 min at room temperature, removed from the thoracic cavity, and fixed overnight at 4°C. Lungs were embedded in paraffin, cut into serial 5-μm sections, and collected on Superfrost Plus microscope slides (VWR, West Chester, PA).

In Situ Hybridization and Histochemistry

The presence of Muc5ac mRNA and mucin glycoproteins was analyzed in consecutively sectioned tissue samples. *In situ* hybridization was performed on deparaffinized tissue sections according to established protocols (24). The clone used to synthesize sense and antisense riboprobes for the murine Muc5ac cDNA was generated by PCR using the primer pairs for Genbank accession number L42292 (*see* Table 1) to amplify cDNA from mouse stomach. The PCR product was cloned into PCRII-TOPO (Invitrogen), and sequencing confirmed that it encoded 1.9 kb of the 3′ end of mouse Muc5ac. Plasmids were linearized and either T7 (antisense) or SP6 (sense) RNA polymerase was used to generate riboprobes labeled with [α-^{35}S]UTP. Labeled probes were hydrolyzed to generate $\sim$ 300-bp fragments, and samples were overlaid with 8 million counts of antisense or sense riboprobe and hybridized overnight at 60°C. Posthybridization washes were performed as described (24), and slides were dipped in Kodak NTB-2 emulsion and exposed for 1–4 wk. Slides were washed again and counterstained with Hoechst 33258 (Molecular Probes, Eugene, OR) to label nuclei. *In situ* labeled sections were viewed by darkfield fluorescence microscopy and photographed using an Olympus BX60 microscope equipped with a SPOT digital camera (Diagnostics Instruments, Sterling Heights, MI). For fluorescent detection of mucin glycoproteins, serial slides with tissues adjacent to those used for *in situ* hybridization were stained using periodic acid fluorescent Schiff's (PAFS) staining (5). All slides were dehydrated in graded ethanol solutions, air dried, and coverslipped with Canada balsam mounting medium (50% Canada balsam resin, 50% methyl salicylate; Fisher Chemicals, Pittsburgh, PA).

Genomic DNA Cloning and Sequence Analysis

The 5′ end of the coding region of the mouse Muc5ac gene was analyzed by sequence alignment of a mouse bacterial artificial chromosome (BAC; Genbank Acc. No. AC020817) sequence with the 5′ cDNA end of human MUC5AC identified previously (25). This sequence of four putative exons of the 5′ end of mouse Muc5ac was confirmed by RT-PCR of mouse lung cDNA harvested 3 d after antigen challenge using the high-fidelity proofreading polymerase Pfu Turbo (Stratagene, La Jolla, CA) with the Muc5ac cDNA primers described above (*see* Table 1). The 416-bp product matched the putative mouse cDNA sequence and contained a conserved translation start site. A second 2.2-kb product, amplified from contaminating genomic DNA, was used to confirm the exon–intron junctions within this small 5′ segment of Muc5ac.

A 400-bp sequence fragment of the 5′ cDNA end of human MUC5AC corresponding to the mouse 5′ coding region fragment identified above was used to query all current mammalian genomic databases, including mouse (Build 36.1), rat (Build 4.1), cat (Build 1.1), dog (Build 2.1), sheep (Build 1.1), pig (Build 1.1), cattle (Build 3.1),

TABLE 1. PRIMERS USED IN THE CURRENT STUDIES

Experiment	Sequence	Genbank Source
RT-PCR		
Muc2	Sense 5′-TCC AGA AAG AAG CCA GAT CC	AF016695
	Anti 5′-ACA CTG CTC ACA GTC GTT GG	
Muc5ac	Sense 5′-ACA TTT CCC CAT GCT CCA CAG C	AJ511870
	Anti 5′-GTG GTG GTA TTA GAC TCC TGG	
Muc5b	Sense 5′-TTA CAC CTG GCA CAC AAT GG	NM_028801
	Anti 5′-TCC AGC TTC TGC AAG TTT CC	
Muc6	Sense 5′-GCT GTT GCT GCT CTT CAG G	NM_181729
	Anti 5′-GGG CAT ATC TGG TCT TCA GG	
Muc19	Sense 5′-CAG ACT CAC TCC CAC CAA CC	AY570293
	Anti 5′-TTA ACG GTC ACG TTC ACA GG	
qPCR		
Muc2	Sense 5′-TGA TGA GAT CTG CAA GTC TTG TAC AT	XM_620587
	Anti 5′-TGT TAA GAA TCT TCC CTT CAT CTG G	
	Probe 5′-CAC CAA CAC GTC AAA AAT CGA ATG CCA	
Muc5ac	Sense 5′-AGA ATA TCT TTC AGG ACC CCT GCT	AJ511870
	Anti 5′-ACA CCA GTG CTG AGC ATA CTT TT	
	Probe 5′-CTC AGC GTG GAG AAT G	
Muc5b	Sense 5′-CAT CCA TCC CAT TTC TAC CAC AA	NM_028801
	Anti 5′-AGG CAA CAT AGA GTT GCT TTT GG	
	Probe 5′-ACA ACC AAG AAC CCT CAA ACA CTA GTC AC AG	
Muc19	Sense 5′-GCA ACC CCA CAG GCT TAG TG	AY570293
	Anti 5′-TTT GAA TCG TAG ATT CTC TCT TCT TCT G	
	Probe 5′-TCA GGA CTG CCC AAA GCA AAC ATG G	
CCSP	Sense 5′-CCT TTC AAC CCT GGC TCA GA	X67702
	Anti 5′-AGG GTA TCC ACC AGT CTC TTC AG	
	Probe 5′-CAA AAT GCG GGC ACC CAG	
Clca3	Sense 5′-GGC ATC GTC ATC GCC ATA G	NM_017474
	Anti 5′-CAC CAT GTC CTT TAT GTG TTG AAT G	
	Probe 5′-CAC GAC GTG CCG GAA GAT GAA GC	
ChIP	Sense 5′-CTG CCA TTG ACT AGC CTG AA	AC020817
	Anti 5′-CAC TGG CAG CCT CTG AGG AA	
In situ Hybridization		
Muc5ac	Sense 5′-ATG TCA TCT CCT TGA GCC CAC G	L42292
	Anti 5′-TGC ACC GTA CAT TTC TGC TG	
Promoter Analysis		
−1 kb	Sense 5′-AGG GCA GTA CAG AGA ACC AC	AC020817
−2 kb	Sense 5′-GTC TTG TCT GTG ATC TGG TC	
−3 kb	Sense 5′-CAG AGG ATC ATG GAG TCT TG	
−4 kb	Sense 5′-TAT GGC TAT GGG CTA GAA GTG G	
−5 kb	Sense 5′-AGG ATC CAA ACA GCA GGT CC	
	Anti 5′-GCT GTG GAG CAT GGG GAA ATG	

and chimpanzee (Build 2.1), using a cross-species discontiguous MegaBLAST alignment. Positive queries were identified in the mouse, dog, and cattle genome assemblies. To determine the overall conservation of these orthologs within their amino terminal coding regions, sequences were further analyzed using EMBOSS pairwise and ClustalW multiple alignment tools. Next, all available upstream sequences from mouse, dog, cattle, and human (including some gaps in the chromosome contigs) between the start codon for MUC5AC and the stop codon for MUC2 (the adjacent gene 5′ to MUC5AC) were retrieved from the available GenBank nucleotide databases. These were analyzed as described above for the 5′ coding regions. To obtain a putative transcription factor (TF) binding profile for mouse Muc5ac with relevance to that of the human gene, a TRANSFAC database analysis was performed on both the mouse and human sequences using Matinspector (www.genomatix.de; 26). This sort of analysis is inherently error prone, so the matrix thresholds were set to $\geqslant$ 90%. The putative TF profile was further narrowed using rVista (rvista.dcode.org), which specifically cross-references primary sequence homologies determined by BLASTz alignment with the TRANSFAC database (27–29), and thus allows for identification of highly conserved TF binding sites within orthologous gene sequences (30).

Construction of Muc5ac Promoter Luciferase Constructs

PCR of the BAC was used to generate 1- to 5-kb genomic DNA fragments containing the 5′ flanking region of mouse Muc5ac at 1-kb increments. PCR was performed using Pfu Turbo, and the primer sequences used are shown in Table 1. The antisense primer was positioned directly adjacent to the translation start site. The resulting amplicons were first cloned into pCRII-TOPO Blunt vector and then subcloned into pGL3 Basic firefly luciferase reporter vector (Promega, Madison, WI) using HindIII and XhoI sites in the PCRII and pGL3 for the 1-, 2-, and 3-kb promoter constructs and the HindIII and SpeI sites in PCRII-TOPO and HindIII and NheI sites in pGL3 for the 4- and 5-kb constructs. To study the effects of specific TF consensus motifs on Muc5ac promoter function, the 1-kb promoter construct was mutated at specific sites using the Quick Change XL Site Directed Mutagenesis kit (Stratagene). A pGL3 reporter construct containing 800 bp of the mouse CCSP promoter was generated previously (31). For chimeric promoter constructs testing the specificity effects of −2/−3 kb repressor domain of the Muc5ac promoter on CMV promoter activity, the luciferase cDNA from pGL3 Basic was first subcloned into pCDNA 3.1 Hygro (Invitrogen) and the −2/−3 kb Muc5ac region was then cloned 5′ to the CMV promoter using the endogenous MluI site present in the distal 5′ end of the CMV promoter in pCDNA 3.1 and PCR generated MluI sites in the Muc5ac fragment. For chimeric Muc5ac −2/−3 kb-CCSP promoter constructs, the CMV site was withdrawn from the pCDNA 3.1 CMV-luciferase construct using MluI and HindIII, and the −2/−3 kb domain was cloned in using PCR generated MluI and HindIII sites on the 5′ and 3′ primers, respectively.

Cell Lines and Transfection

Experiments testing Muc5ac and CCSP promoter activation were performed in a mouse transformed Clara cell line (mtCC1–2) (23), in 3T3 fibroblasts (ATCC, Manassas, VA), and in two human lung adenocarcinoma cell lines, NCI-H292 and A549 (ATCC). Cells were co-transfected with firefly luciferase-promoter constructs along with the Renilla luciferase control vector pRL-TK (Promega) to normalize for transfection efficiency. A quantity of 1–2 $\times$ 10^5 cells was seeded on 6-well plates and were co-transfected 24–48 h later with test promoter and pRL-TK using Fugene 6 (Roche, Indianapolis, IN). Because of the varying sizes of the promoter constructs used in these studies, cells were transfected with equimolar quantities of test promoter (50 or 200 mmol as indicated), and empty self-ligated pCRII was added to each transfection mixture along with either 30 or 100 ng of pRL-TK to raise the final mass of DNA per well to 0.3 or 1 μg, respectively. Experiments testing the activation of the Muc5ac promoter in response to cytokine stimulation were performed in mtCC1–2's. To determine the effects of cytokine stimulation on promoter activity, cells were seeded, grown, and transfected as above and then serum starved for 6 h, followed by 24 h incubation with media containing 100 ng/ml of recombinant mouse IL-13 (the kind gift of Dr. D. Donaldson, Wyeth Research, Cambridge, MA) or 25 ng/ml of recombinant mouse EGF (Peprotech, Rocky Hill, NJ). In preliminary studies, we found that EGF and IL-13 significantly increase Renilla luciferase activity in cells transfected with pRL-TK alone. Therefore, when Muc5ac promoter responsiveness to EGF, IL-13, and medium alone was compared here, data were normalized to total protein content in cell lysates determined by bicinchoninic acid (BCA) assay (Pierce, Rockford, IL). Transient transfection experiments were performed in triplicate or sextuplicate and repeated on at least three occasions, and the data are presented as the means of firefly luciferase activity normalized to Renilla luciferase activity or protein mass as noted.

Chromatin Immunoprecipitation

Chromatin immunoprecipitation (ChIP) was used to determine the biochemical interactions of transcription factors with the Muc5ac promoter. Experiments were performed using the ChIP-IT kit (Active Motif, Carlsbad, CA) according to the manufacturer's instruction. Briefly, cells were grown on 15-cm tissue culture plates grown to $\sim$ 75% confluence and stimulated with EGF and IL-13 as described above. After overnight incubation, cells were fixed for 10 min in 10% formalin, lysed, and nuclease treated. Immunoprecipitation was performed using rabbit polyclonal antibodies to HIF-1α (Novus Biologicals, Littleton, CO) and SMAD4 (Santa Cruz Biotechnology, Santa Cruz, CA). Nonspecific rabbit IgG (Santa Cruz Biotechnology) was used as a negative control. Primary and control antibodies were incubated with digested tissue culture lysates overnight at 4°C under constant rotation at a final concentration of 3 μg per 170 μl reaction. Antibody–antigen complexes were then incubated with protein G–linked goat anti-rabbit IgG and precipitated by centrifugation at 20,000 $\times$ *g* for 15 min at 4°C. Aliquots of input DNA not exposed to primary or secondary antibodies were stored separately for normalization. Immunoprecipitated DNA was analyzed by PCR using primers that flank the core promoter region (sense primer, −144 to −125 bp in Muc5ac gDNA sequence; antisense primer +20 to +1 in Muc5ac gDNA sequence; *see* Figure 4 for gene references and Table 1 for primer sequences). PCR products were initially analyzed by agarose gel electrophoresis to determine reaction efficiency and the absence of detectable primer dimer amplification. Quantitative PCR was then performed using the same primer set with SYBR green detection (Quantitect; Qiagen, Valencia, CA). Standard curves were generated using linearized plasmid DNA containing the 1-kb wild-type mouse Muc5ac promoter, and the dynamic range of sensitivity ranged from 1 copy to 10^9 copies.

Statistical Analysis

Quantitative data are presented as means ± SE, and statistical analysis was performed using Student's *t* test (Statistica, Version 6.1; StatSoft Inc., Tulsa, OK). A P value of ≤ 0.05 was considered significant.

RESULTS

Muc5ac Is Selectively Up-Regulated in the Lungs of Antigen-Challenged Mice

To identify which mucin genes are involved in the development of allergic mucous metaplasia, we measured the expression levels of the complete set of murine gel-forming mucin genes at baseline and over a 1-wk period after a single aerosol antigen challenge. In the absence of antigen challenge, very little histochemically detectable mucin glycoprotein is found in the nonciliated epithelial cells of mouse conducting airways (Figure 1A). By contrast, sensitized mice exposed to a single aerosol ovalbumin challenge develop a prominent mucous phenotype within the airway epithelium that is apparent within 24 h and is maximal at 3–7 d (Figure 1B and Ref. 5). A nonquantitative RT-PCR survey of gel-forming mucin genes at these time points reveals that only Muc5ac, Muc5b, and scant Muc19 transcripts are present at baseline or after antigen challenge (Figure 1C). No detectable Muc2 or Muc6 transcripts were found at any time points assessed

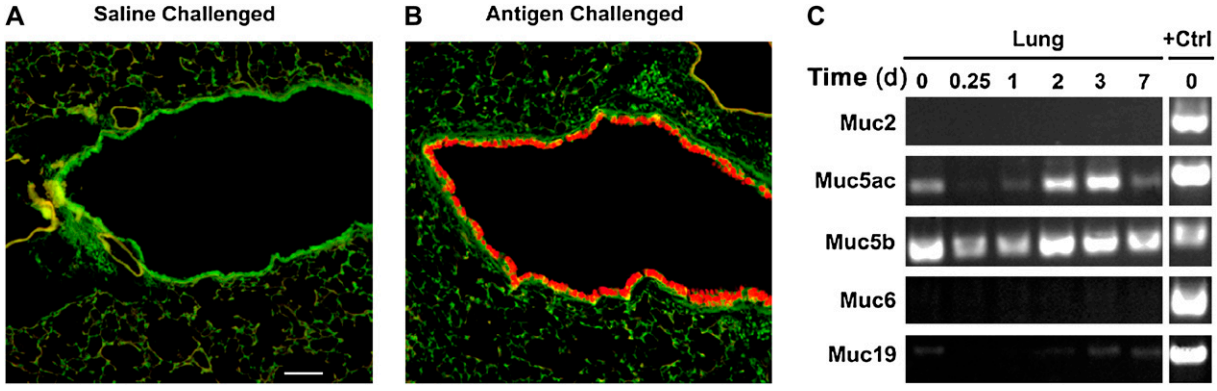

Figure 1. A single antigen challenge causes goblet cell metaplasia and alters mucin gene expression in sensitized mice. (*A*) The airway epithelium of saline challenged mice contains few or no PAFS-positive mucin granules. (*B*) Three days after antigen exposure, the airways demonstrate an increase in PAFS-positive mucin granules (red). (*C*) RT-PCR analysis of gel-forming mucin genes over a 1-wk time course of goblet cell metaplasia after a single antigen challenge demonstrates that Muc5ac, Muc5b, and scant Muc19 are detectable at baseline and after antigen challenge while no Muc2 or Muc6 are detectable at any time points. *Magnification bar* = 50 μm for *A* and *B*. Positive controls in *C* are PCR of reverse-transcribed total RNA extracted from colon (Muc2, 1,046 bp), stomach (Muc5ac, 414 bp and Muc6, 791 bp), tongue (Muc5b, 512 bp), and salivary gland (Muc19, 451 bp). Data are single representatives of samples from 5–12 mice per group.

qualitatively here (Figure 1C). Next, to quantitatively determine which of these are expressed coincidentally with histochemically detectable mucin glycoprotein, we measured the expression of Muc5ac, Muc5b, and Muc19 by qRT-PCR (Figure 2). Muc5ac and Muc5b mRNAs are detectable even in the absence of histochemically detectable goblet cells at baseline (138 and 3,994 mRNA copies per 10^6 18S rRNA copies, respectively). Moreover, both are expressed at significantly higher levels than either Muc2 (14 mRNA copies per 10^6 18S rRNA copies) or Muc19 (5 mRNA copies per 10^6 18S rRNA copies). After antigen challenge, Muc5ac is the predominant mucin gene induced. It increases 7-fold 2 d after challenge (966 mRNA copies per 10^6 18S rRNA copies) and $>$ 40-fold 3 d after challenge (5,970 mRNA copies per 10^6 18S rRNA copies). In contrast to the robust induction of Muc5ac transcription, Mucs 2, 5b, and 19 transcripts do not increase in a statistically significant manner. In fact, they are reduced by 45–70% compared with baseline 2 d after challenge, and they only increase 2- to 5-fold 3 d after challenge. Thus, both Muc5ac and Muc5b are present within the lungs of mice at baseline and after antigen challenge, but it is the up-regulation of Muc5ac that corresponds with the dramatic increase in histochemically detectable mucin present within the epithelium after challenge.

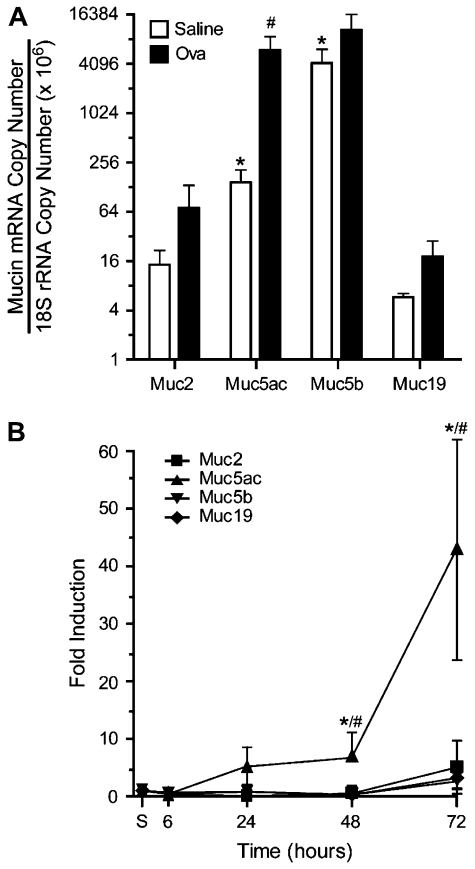

Figure 2. Muc5ac is selectively induced in the lungs of antigen-challenged mice. (*A*) Quantitative RT-PCR of total lung RNA demonstrates predominant Muc5b mRNA at baseline (*open bars*). Muc5ac mRNA is present at $\sim$ 30-fold lower levels than Muc5b while Muc2 and Muc19 mRNAs are present at $\sim$ 300 and $>$ 700-fold lower levels than Muc5b, respectively. Three days after antigen challenge (*filled bars*), Muc5ac is the only gel-forming mucin whose mRNA levels increase significantly. (*B*) The magnitude of Muc5ac induction, compared with its expression level in saline-challenged mice (S), is significant 72 h after exposure, but not at earlier time points. Muc5ac (*upright triangles*) induction is also of significantly greater magnitude than any changes seen in Muc2 (*squares*), Muc5b (*inverted triangles*), or Muc19 (*diamonds*) mRNA levels at any time points studied here. Data are presented as means $\pm$ SE of triplicate samples from 5–12 mice per group. *Significant difference from other mucin mRNAs within a given treatment group/time point. #Significant difference between an individual mucin and its baseline expression level. Note Log2 scale for *y* axis in *A*.

Muc5ac Expression Is Localized to a Subset of Proximal Airway Epithelial Cells

To identify the localization of Muc5ac expression in the lungs of mice, *in situ* hybridization was performed. Muc5ac mRNA is expressed within the airway epithelium of antigen-challenged mice, but it is undetectable within the airway epithelium of unchallenged controls (Figure 3). Moreover, Muc5ac expression localizes to the central bronchial airways but is absent in the peripheral bronchiolar airways. This expression pattern matches that of intracellular mucin glycoprotein content detected by PAFS staining, demonstrating that mRNA synthesis levels are tightly associated with protein synthesis levels.

Identification of Conserved Putative TF Binding Motifs within the Muc5ac Promoter

Having shown that Muc5ac is the most highly induced gel-forming mucin gene during allergic goblet cell metaplasia *in vivo*, we analyzed the upstream 5′ flanking region to test for evolutionary conservation of potential functional regulatory elements that may drive Muc5ac expression. We previously cloned the 5′ coding sequence and 1-kb of the 5′ flanking region of mouse Muc5ac (5). Alignment of these mouse sequences with other known mammalian sequences shows high homology among orthologs (60–90% within the coding region and 60–80% within the proximal 5′ flanking region). Among the most highly conserved domains are the coding sequence for the amino terminal von Willebrand factor D–like domain ($>$ 95%) and several recognition motifs for TF binding within the core promoter (Figure 4).

In all mammalian genomes mapped in the 11p15 syntenic region thus far, the clustered gel-forming mucins are present in the following locus order (centromere $\rightarrow$ telomere): 5′-MUC6 (complementary strand) $\rightarrow$ MUC2 $\rightarrow$ MUC5AC $\rightarrow$ MUC5B-3′. We therefore scanned the full 5′ intergene sequence between the coding regions of mouse Muc2 and Muc5ac ($>$ 34 kb), rat Muc2 and Muc5ac ($>$ 12 kb), dog MUC2 and MUC5AC ($>$ 24 kb), cattle MUC2 and MUC5AC ($>$ 42 kb), chimpanzee MUC2 and MUC5AC ($>$ 40 kb with gaps), and human MUC2 and MUC5AC ($>$ 47 kb) to search for ECRs that harbor TF consensus motifs. We next examined the 5′ flanking regions of these MUC5AC orthologs, using rVista. The rVista software tool generates a BLASTz alignment (27–29) that is weighted toward analysis of two highly divergent sequences such as noncoding genomic DNA regions, and then identifies ECRs and cross-references these against the TRANSFAC database to determine whether putative functional TF-binding sites are present in both species (30). The 5-kb region proximal to the translational start site contains the highest degree of conservation among species (mouse versus human shown in Figure 5). Our analysis identifies 16–18 ECRs that contain clusters of $\geq$ 100 bp with at least 70% homology between humans and cattle and humans and mice. Likewise, there are 31–39 ECRs that contain clusters of $\geq$ 20 bp with at least 90% homology between humans and cattle and between humans and mice. TRANSFAC analysis of these reveals conservation of SMAD4, HIF1/NMYC, and FOXA2 binding sites within the 1-kb domain proximal to the translational start site, as well as conservation of a site for NKX2.5 (a relative

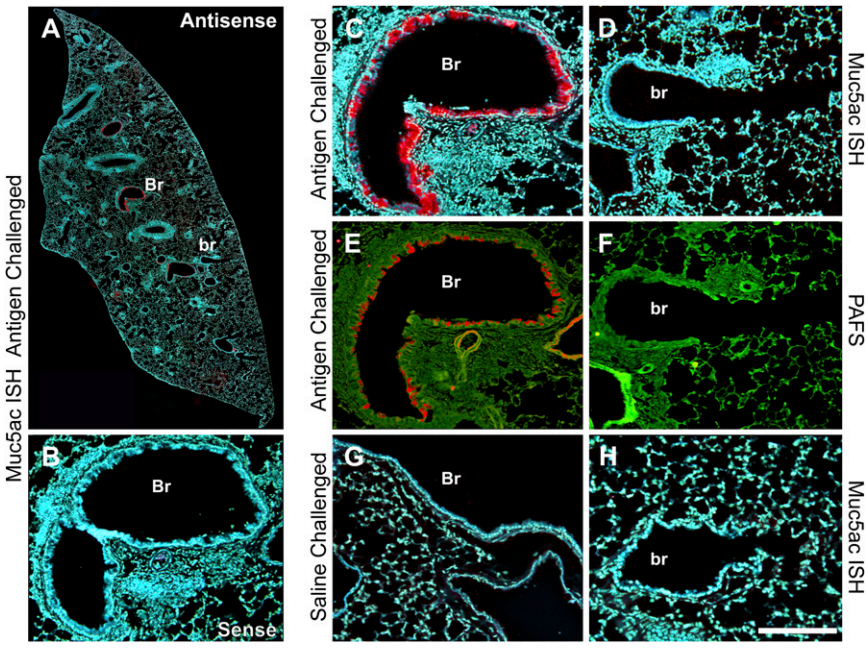

Figure 3. Coordinate expression of Muc5ac mRNA and PAFS-positive mucin staining within the bronchial epithelium of antigen-challenged mice three days after single antigen challenge. *In situ* hybridization was used to detect Muc5ac mRNA in lung sections from antigen-challenged (*A–D*) and saline-challenged (*G* and *H*) mice. The antisense Muc5ac riboprobe hybridizes to the epithelium in the bronchial (Br) airways (*red* in *A* and *C*), but not in the bronchiolar (br) airways (*A* and *D*). PAFS staining of a consecutive airway section shows mucin (*red* in *E*) in the same cells of the bronchial airways that show Muc5ac mRNA positivity in *A* and *C*. No PAFS-positive mucin staining is present within epithelium of the bronchiolar airways (*F*) that also showed no Muc5ac mRNA (*D*). Lack of signal detection after incubation with sense riboprobe in the opposite consecutive antigen-challenged lung section as that shown in *E* and *F* (*B*) or incubation with antisense riboprobe in lung sections of saline challenged animals demonstrates specificity of the findings in *A*, *C*, and *D*. *Magnification bar* = 100 μm. *Blue* in *A–D*, *G*, and *H* is Hoechst 33258. *Green* in *E* and *F* is intercalated acriflavine staining of nuclear and cytoplasmic nucleic acids.

of NKX2.1, or TTF-1, a ubiquitous airway epithelial cell TF) in the −1/−2 kb region (Figure 5). Manual identification of high stringency MatInspector hits identifies additional sites including the following: additional SMADs and the zinc-finger SMAD inhibitor transcription factor (TCF) 8, both TGF-β–signaling effectors (32); lymphoid enhancer binding factor 1 (LEF1), the major downstream target of β catenin (33); and basic kruppel like factor (BKLF/KLF3), a TF whose relative (lung KLF or LKLF/KLF2) shares the same recognition motif and was recently shown to be up-regulated in smokers with moderate chronic obstructive pulmonary disease (COPD) (34).

To test the function of the conserved promoter elements identified above, we developed an *in vitro* system that models characteristics of murine mucous metaplasia. We used mtCC1–2s, which were established previously by Magdaleno and coworkers who cultured epithelial cells from the tumors of transgenic mice expressing SV40 Large T Antigen under control of the CCSP promoter (23). We grew mtCC1–2s in the presence and absence of IL-13 or EGF, two cytokines that activate signal transduction pathways known to be required for the development of mucous metaplasia *in vivo*. The expression of Mucs 2, 5ac, 5b, and 19, as well as the metaplastic marker calcium-activated chloride channel (Clca)-3 and the baseline Clara cell marker CCSP, were measured by performing qPCR on cDNA from control and IL-13– or EGF-stimulated cultures (Figure 6A). In the absence of these cytokines, none of the mucins tested here are detectable, but CCSP and Clca3 are (38 and 1,158 mRNA copies per 10^6 18S rRNA copies). However, upon cytokine stimulation, there is a marked up-regulation of Muc5ac (14 and 53 mRNA copies per 10^6 18S rRNA copies with IL-13 or EGF, respectively) with no significant changes in Mucs 2, 5b, or 19 (Figure 6). Likewise, these two cytokines also significantly induce Clca3 expression to 24,086 (> 20-fold, IL-13) and 5,033 (> 4-fold, EGF) copies. IL-13 (but not EGF) also induces Muc5b expression, but this effect did not achieve statistical significance ($P = 0.08$). At the protein level, PAFS-positive cells are present in the core regions of lungs tumors (< 10%) in transgenic mice expressing SV40 Large T Antigen under control of the murine CCSP promoter (Figures 6B and 6C), suggesting that our findings of transcript regulation are associated with mucin glycoprotein production. Collectively, these data reflect what is seen in control and antigen challenged mice *in vivo*, since mtCC1–2s exhibit regulated expression of components of the *in vivo* mucous metaplastic phenotype *in vitro*.

Control of Muc5ac Induction by Conserved 5′ Elements

Having established regulated expression of mucous metaplastic markers in mtCC1–2s, we next used them as a proxy to identify *cis* and *trans* factors that potentially mediate Muc5ac gene regulation with the potential to regulate gene activity. To this end, we first analyzed the effects of conserved Muc5ac 5′ noncoding region on luciferase activity in reporter assays *in vitro*. We cloned 1-, 2-, 3-, 4-, and 5-kb fragments of the 5′ flanking region adjacent to the translational start site, generated promoter–luciferase reporter constructs, and tested their relative activities in murine transformed Clara cells (mtCC1–2s) and fibroblasts (3T3 cells). When transfected into mtCC1–2s, luciferase activity was highest when driven by the 1- and 2-kb promoters, but luciferase activity was abolished when driven by the 3-, 4-, and 5-kb promoters (Figure 7). In these cases, reporter activity fell below even the baseline leak of the "promoterless" pGL3 Basic vector. By contrast, there was little or no luciferase activity in 3T3 fibroblast cells. These results demonstrate that the first kb of the mouse Muc5ac promoter confers robust levels of transcriptional activation, and they suggest that it also confers some degree of epithelial, in this case Clara cell, selectivity. They further show that a strong repressor element is present within the third kb upstream of the Muc5ac gene (the −2/−3 kb domain), and this renders the Muc5ac promoter virtually inert within both mtCC1–2 and 3T3 cells. In a small number or experiments we also tested activation of the mouse Muc5ac promoter A549 and NCI-H292 cells. These human lung adenocarcinoma cell lines produce MUC5AC at both the message and protein levels. In these cells, the mouse Muc5ac promoter drives a strikingly similar pattern of reporter activity (*see* Figure E1 in the online supplement).

To further test the context of −2/−3 kb domain–mediated repression, we used chimeric promoter constructs with a 1-kb fragment representing the entire −2/−3 kb repressor domain of

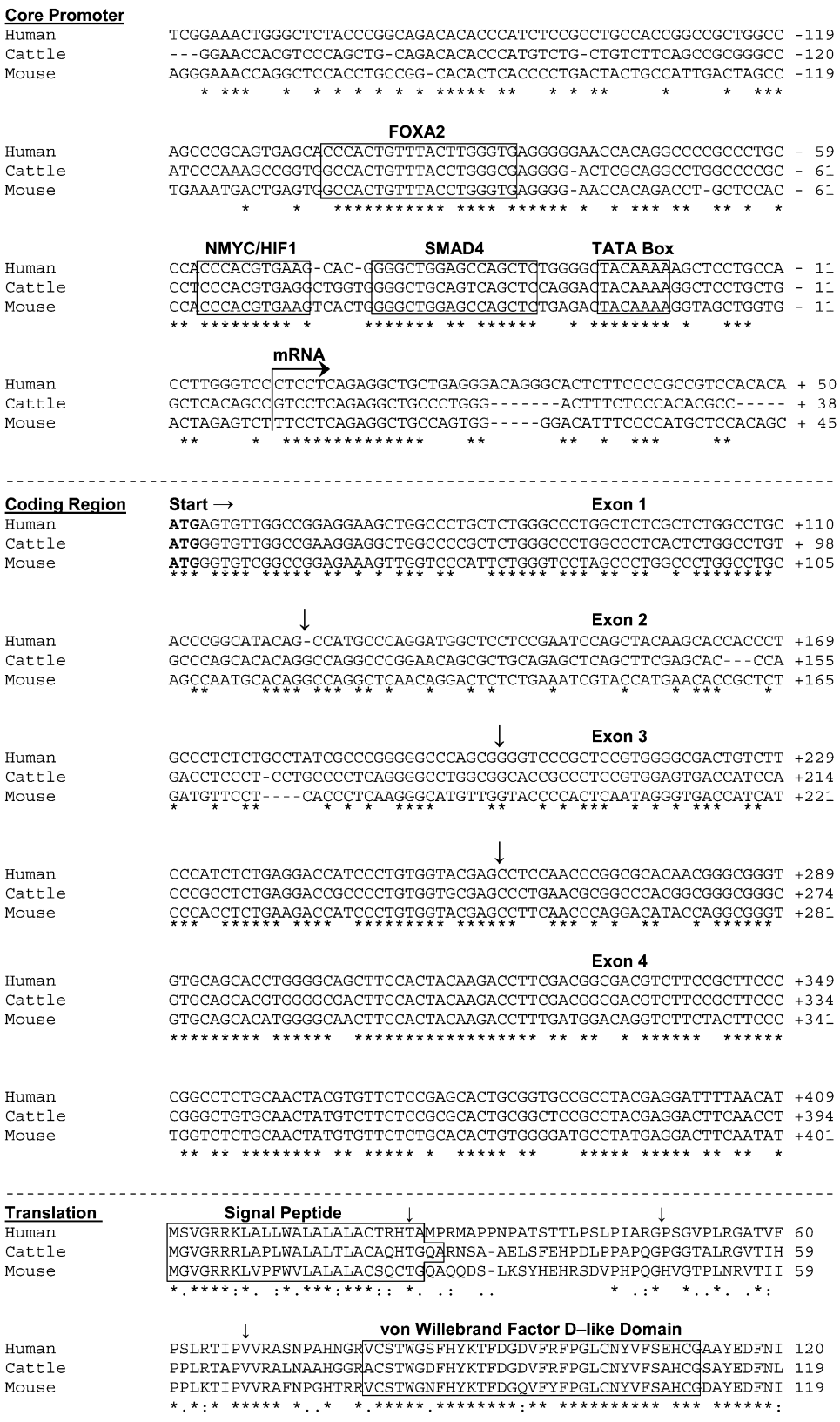

Figure 4. Alignment of 5′ noncoding, coding, and translated sequence fragments of mammalian MUC5AC orthologs. (*Top section*) The ∼ 200-bp segment of the 5′ flanking region proximal to the conserved transcriptional initiation site (*arrow*) shows 55% cross-species identity and conserved consensus sequences for TFs (*boxed segments*). (*Middle section*) The ∼ 360 bp four exon amino terminal coding cDNA segments show 65% cross-species identity. (*Bottom section*) Translation of the four-exon segment above shows a conserved signal peptide and a highly conserved von Willebrand Factor D–like Domain that is a characteristic of the amino termini of all gel-forming mucins. *Inverted arrows* depict exon junctions.

the mouse Muc5ac 5′ flanking region fused in *cis* 5′ to the mouse CCSP promoter (∼ 800 bp) or to the CMV promoter (∼ 600 bp) in luciferase reporter vectors. When transfected into mtCC1–2s, CMV promoter activity was unaffected by the presence or absence of the Muc5ac −2/−3 kb repressor domain (Figure 8). By contrast, CCSP promoter activity was abolished in the presence of the Muc5ac −2/−3 kb repressor domain. Collectively, these results demonstrate that multiple domains within the 5′ flanking region of the Muc5ac gene specify the cellular context of Muc5ac gene expression *in vitro*. Furthermore, our data suggest that at

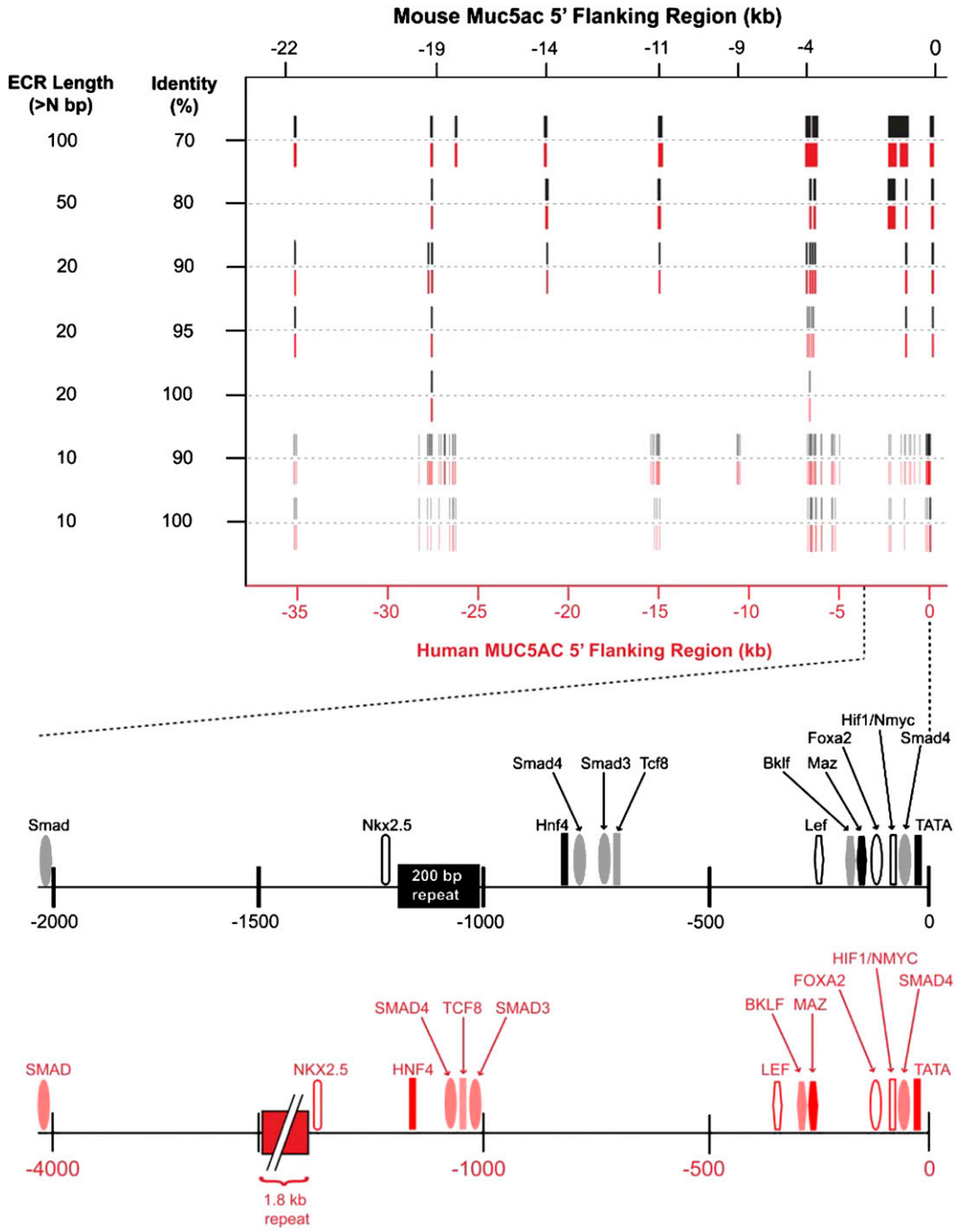

Figure 5. Evolutionary conservation of the 5′ flanking region of mouse and human MUC5AC orthologs. (*Top*) Evolutionarily conserved regions (ECRs) within the MUC2–MUC5AC intergene sequences of mice (*black*) and humans (*red*) were identified using BLASTz alignment to show the presence of discrete blocks of ECRs. ECRs are most frequent in the proximal promoter-enhancer regions (~ 7 kb in humans and ~ 5 kb in mice). (*Bottom*) rVISTA analysis shows conservation of TF consensus sequences in mouse (*black*) and human (*red*) proximal promoters. *Numbers below axes* depict distance (bp) from transcriptional start site.

least one of these domains, the −2/−3 kb repressor domain, functions by a mechanism that is redundant among Clara cell secretory products.

To better understand the mechanisms of core (1-kb) promoter activation, we next made mutations in the evolutionarily conserved TF consensus sites that we identified *in silico*. Singly, mutation of the Nmyc/HIF1 and the SMAD4 consensus sites each significantly disrupts promoter activation in serum-stimulated cells (Figure 9). In combination, mutation of these two sites completely abolishes promoter activity induced in serum-stimulated cells. In addition to these factors, there is small, but statistically significant inhibition of promoter activity in Lef1 consensus site mutants. Together, these data suggest that a significant level of control of the Muc5ac promoter derives from the activation of cellular stress (HIF1), damage (β catenin/Lef1), and remodeling/repair (TGF-β/SMAD) pathways.

To test which domains of the Muc5ac promoter also confer inducible transcriptional activation, we next tested whether IL-13 and EGF, two cytokines that are required for the development of mucous cell metaplasia in animals *in vivo* (6), are likewise capable of inducing Muc5ac promoter activity in mtCC1–2s *in vitro*. Our studies show that the Muc5ac promoter is induced in response to stimulation by these cytokines (Figure 10). Moreover, induction occurs via activation of elements within the first kb of the 5′ flanking region, consistent with what we have shown previously (5). Surprisingly, the 3- to 5-kb region continues to render luciferase activity to levels below baseline despite cytokine stimulation, suggesting that the strong inhibitory −2/−3 kb element

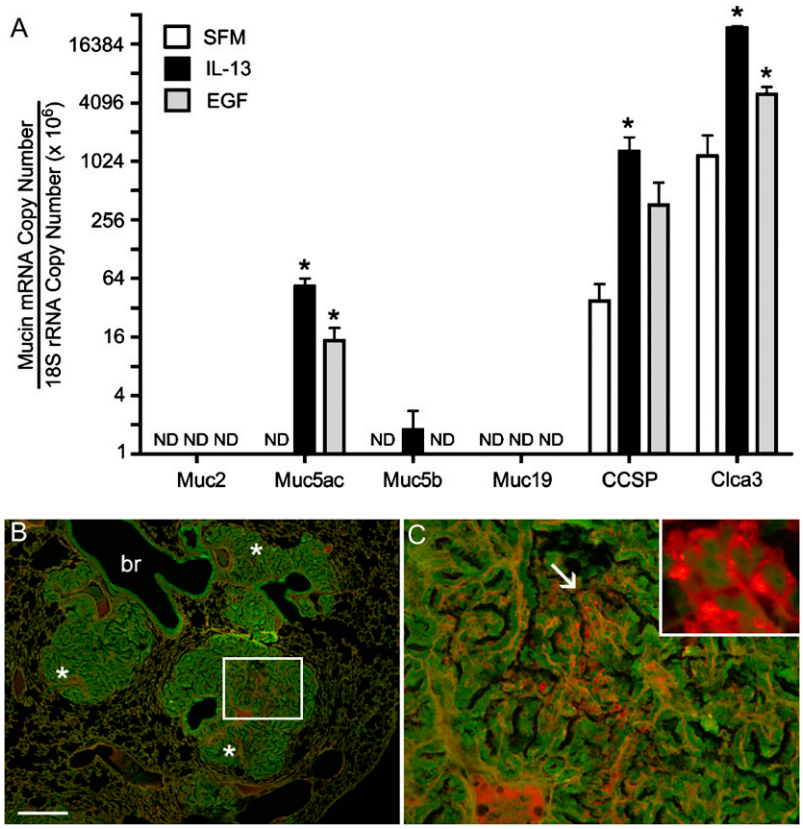

Figure 6. Mouse transformed Clara cells express markers of mucous metaplasia. (*A*) Cultures of mtCC1–2s were serum starved for 6 h and then incubated with IL-13 (100 ng/ml; *black bars*) or EGF (25 ng/ml; *gray bars*) for 24 h. Quantitative RT-PCR was then used to assess Muc2, Muc5ac, Muc5b, and Muc19 mucin mRNAs. CCSP and Clca3 were also assessed as independent markers of baseline and mucous metaplastic gene expression, respectively. Muc5ac, CCSP, and Clca3 (but not Muc2, Muc5b, or Muc19) are significantly increased by IL-13. Only Muc5ac and Clca3 are significantly increased by EGF in mtCC1–2s. Data are means ± SE from three independent experiments conducted in triplicate. (*B*) PAFS staining of a tissue section from a 20-wk-old CCSP-SV40 T Ag transgenic mouse demonstrates the presence of bronchiolar tumors (*white asterisks*), some of which contain mucous cells (*box* in *B* shown at higher magnification image in *C*). *Arrow* in *C* identifies a region of PAFS-positive papillary tumor growth shown in the inset. *Magnification bar* = 150 μm (*B*), 30 μm (*C*), and 10 μm (*inset*). Note Log2 scale for *y* axis in *A*. *Significant difference between an individual mRNA and its baseline expression level.

described above overpowers the activation of the proximal promoter regions in this *in vitro* setting. Having identified core HIF-1 and SMAD4 TF motifs as critical sites for promoter activity in the −1 kb promoter region in serum-treated cells, we next tested whether IL-13 or EGF-induced promoter activity functions through use of HIF-1 and SMAD4 TF motifs. In HIF-1 and SMAD4 TF motif mutant-transfected cells stimulated with IL-13 or EGF, luciferase activity fails to increase above the level seen in unstimulated or cytokine-stimulated cells transfected with the wild-type promoter (Figure 11). Furthermore, mutation of both sites in combination causes a further decrease in luciferase activity after cyokine stimulation (Figure 11). In cells transfected with SMAD4 and HIF-1 mutant constructs, there is also a ∼ 50% decrease in luciferase activity in cells cultured in serum-free medium (SFM) alone compared with cells transfected with the wild-type promoter and cultured in SFM simultaneous parallel

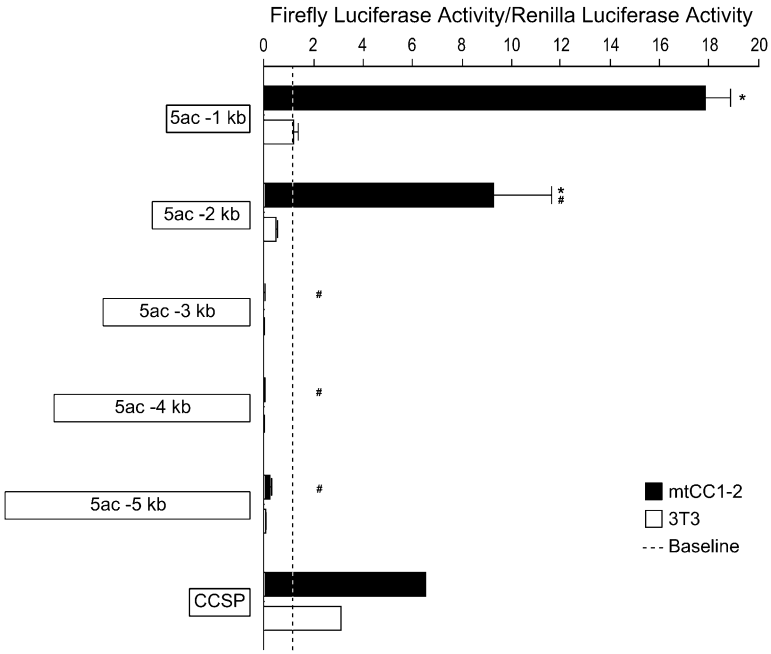

Figure 7. Muc5ac promoter activity in mouse transformed Clara cells. 1–5 kb Muc5ac promoter-luciferase constructs were transfected into mtCC1–2's (*black bars*) and 3T3 cells (*white bars*) and incubated overnight in serum supplemented medium. The 1 and 2 kb domains proximal to the translation start site are strongly activated in mtCC1–2s, but not 3T3 cells. By contrast, inclusion of distal domains (3–5 kb upstream) abolishes luciferase activity. Like the Muc5ac promoter, the 800-bp core promoter of CCSP also directs Clara cell–selective transcriptional activation. *Dashed line* is luciferase activity in cells transfected with empty pGL3 vector. Data are presented as means ± SE of triplicate samples from five experiments. *Significant difference from 3T3 cells, and #significant difference from 1 kb promoter activity in mtCC1–2s.

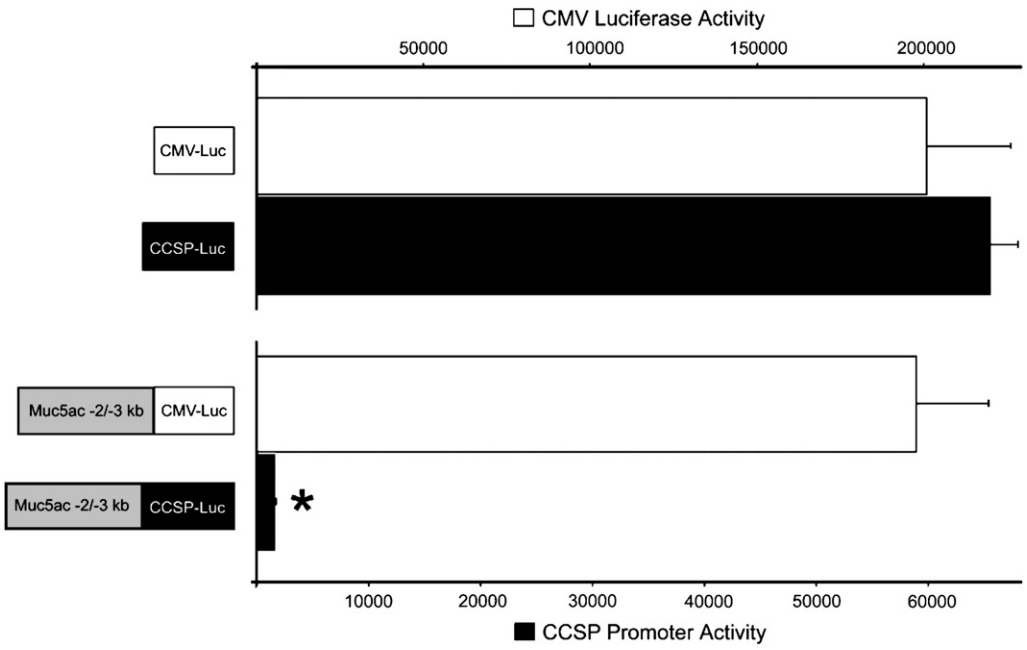

Figure 8. The third (−2/−3) kb domain of the 5′ flanking region of Muc5ac contains repressor(s) that act redundantly upon Clara cell secretory products. (*Top*) mtCC1–2s were transfected with constructs containing either CMV (white bar) or CCSP (black bar) promoter driven luciferase and incubated overnight in serum supplemented medium, and these direct high levels of luciferase activity. (*Bottom*) Chimeric promoter constructs in which the −2/−3 kb repressor domain of the Muc5ac 5′ flanking region is present 5′ to CMV (*white bar*) or CCSP (*black bar*) promoter driven luciferase show uninhibited CMV-driven luciferase activity and ablated CCSP promoter-driven luciferase activity. Data are presented as means ± SE of triplicate samples from three experiments. *Significant difference from −2/−3 kb CMV, and nonchimeric CMV and CCSP promoter–driven reporters.

experiments (data not shown). Cells were also transfected with the Foxa2, Maz, Lef, and TCF8 reporter mutants (*see* Figure 9) and incubated in either SFM or SFM supplemented with either IL-13 or EGF. Mutation of these sites causes no changes in either baseline or cytokine stimulated promoter activity (data not shown). Collectively, these data demonstrate that the HIF-1 and SMAD4 *cis* motifs identified here are required for induction of the Muc5ac promoter in response to IL-13 or EGF.

Lastly, we tested whether HIF-1 and SMAD4 are indeed capable of functioning as *trans* acting factors using quantitative ChIP analysis to confirm whether their binding are associated with Muc5ac promoter activation. At baseline, both HIF-1α and SMAD4 associate with the Muc5ac promoter in mtCC1–2s, since anti–HIF-1α and anti-SMAD4 Abs precipitate Muc5ac promoter DNA (Figure 12). Experiments using control IgG to IP Muc5ac promoter DNA were also performed, and in these studies, the amount of DNA detected was $< 0.001\%$ of that detected when DNA was precipitated with anti–HIF-1α or anti-SMAD4 Abs (data not shown). Incubation of cells with EGF significantly increases the binding of HIF-1α and significantly decreases the binding of SMAD4 to the Muc5ac promoter, as demonstrated using qPCR (Figure 12B). IL-13 also decreases SMAD4 association with the Muc5ac promoter, and it appears to induce an increase in HIF-1α association with the Muc5ac promoter, although this did not achieve statistical significance in the experiments reported here ($P = 0.078$).

DISCUSSION

In the current studies, we demonstrate that Muc5ac is the most highly induced gel-forming mucin in the airways of antigen-challenged mice (Figures 1 and 2). Muc5ac mRNA expression increases over the same time course as airway inflammation and goblet cell metaplasia after antigen challenge, and its localization is restricted to the same anatomical sites as histochemically detectable granular mucin glycoprotein staining in the lungs (Figure 3 and Ref. 5). The Muc5ac 5′ flanking region harbors elements that mediate promoter activation in response to IL-13 and EGF (Figures 6 and 10–12), two cytokines that are required for the induction of Muc5ac expression and the development of goblet cell metaplasia *in vivo* (6, 7). This dynamic and highly selective regulation of the Muc5ac gene appears to involve the activation of conserved 5′ elements that mediate gene activation in Clara cells via HIF-1 and SMAD TFs (Figures 4, 5, 11, and 12). Collectively, these data conclusively identify the expression of Muc5ac as the central event in the development of allergic inflammatory airway goblet cell metaplasia, they identify functional 5′ elements that regulate Muc5ac gene expression *in vitro*, and they provide novel insight into the mechanisms that govern its tight temporal and spatial regulation *in vivo*.

While previous studies had demonstrated that Muc5ac is upregulated after antigen challenge, uncertainty over its role versus the roles played by other mucins has persisted over the years as new gel-forming mucins have been discovered (12, 13, 17, 35, 36). Now, after comprehensive analysis, the total number of gel-forming mucin genes present within the human and mouse genomes is five—MUCs 2, 5ac, 5b, 6, and 19. Although this class of genes is grouped together because of striking similarities in the overall structures of the glycoproteins they encode, differences in their central glycosylation domains and polymerization sites impart gene-specific biochemical and biophysical properties that may necessitate tissue-specific expression (Figure E2). For example, Muc2 is not soluble in aqueous solutions, including strong chaotropic salt solutions such as 6 M guanidium chloride (37). Since this is the chief gel-forming mucin present in the intestinal mucous layer, the density and insolubility of Muc2 likely helps to provide a barrier between intestinal epithelial surfaces and the microbial flora within the intestinal tract. The functional importance of its expression in the intestines *in vivo* is highlighted by the finding that mice deficient in Muc2 develop spontaneous colorectal cancer (38). In contrast to the intestinal tract, the presence of large amounts of such an insoluble mucin within airway mucus (which is $\sim 95\%$ water normally) would likely create a viscous and dense mucus layer that would greatly impair mucociliary clearance. Instead, the presence of small amounts

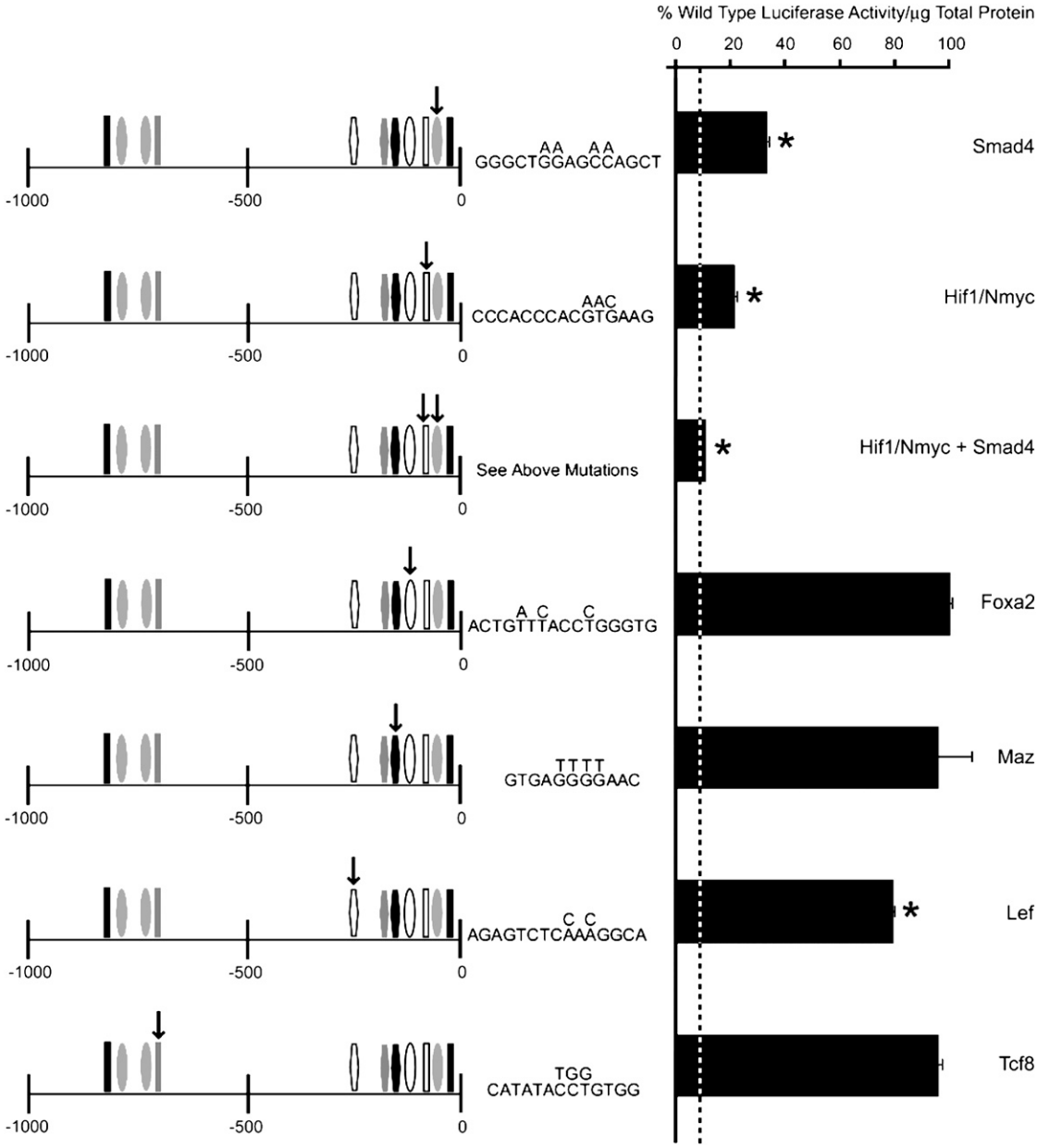

Figure 9. Muc5ac promoter activity is controlled by functional evolutionarily conserved *cis* elements. Site-directed mutagenesis was used to disrupt TF motifs contained within the −1 kb Muc5ac firefly luciferase construct used in Figure 7. Cultures were transfected with 1 μg of DNA and incubated in the presence of 10% fetal bovine serum (FBS) to maximally activate promoter activity overnight. Luciferase and BCA assays were then performed. Data are presented as the percentage of activity of mutated promoters compared with wild type. Mutation of individual Hif1/Nmyc, Smad4, and Lef consensus sites identified *in silico* significantly impairs Muc5ac promoter function *in vitro*. Combined mutation of Hif1/Nmyc and Smad4 sites abolishes promoter activity. *Dashed line* represents baseline wild-type 1-kb Muc5ac promoter activity in the absence of FBS. Values are means ± SE of results from three separate transfection experiments performed in sextuplicate. *Significant difference from wild type.

of the more water-soluble Muc5ac and Muc5b mucins within the airways creates a mucus layer that is viscoelastic (not just viscous), maintains the integrity of the periciliary and mucous gel interface, and thus produces highly efficient mucociliary clearance escalator.

At baseline, Muc5ac and Muc5b transcripts are present in mouse lungs, with Muc5b displaying > 40-fold higher levels than Muc5ac, and in antigen challenged mice, Muc5ac is selectively induced, such that its transcript levels roughly match Muc5b. In endobronchial biopsies and bronchial brushings from human airways, MUC5AC and MUC5B transcript and proteins are both expressed in healthy subjects, and MUC5AC is selectively induced in allergic asthmatics (39) and in smokers with airflow obstruction (40). However, MUC5B expression is lower than MUC5AC at baseline in humans, and its expression decreases in diseased airways (39, 40). Ordinarily, MUC5B is a glandular mucin, and submucosal gland secretions are considered to be important for homeostatic airway hydration and mucociliary clearance in human bronchial (but not bronchiolar) airways. MUC5B may be poorly represented if submucosal glands are not present in biopsied or brushed tissue samples. Mice have submucosal glands only in the upper trachea, and these were not sampled in our current studies. Thus, our finding that Muc5b mRNA is higher than Muc5ac mRNA in mouse lungs (*see* Figure 2) may be related to cross-species anatomical differences that require compensatory changes in gene expression such that Muc5b is enriched in the surface epithelium to maintain airway homeostasis in animals lacking abundant submucosal glands. At baseline, Muc5b mRNA appears to be translated into mature protein, since mice lacking the exocytic regulatory protein Munc13–2 accumulate AB-PAS positive mucin granules in Clara cells that are laden with Muc5b but contain scant Muc5ac (41). In wild-type mice, this goes unnoticed because the levels of histochemically detectable mucin glycoproteins are low compared with the rate of secretion in response to tonic activation of the regulated exocytic pathway. Collectively, these data suggest

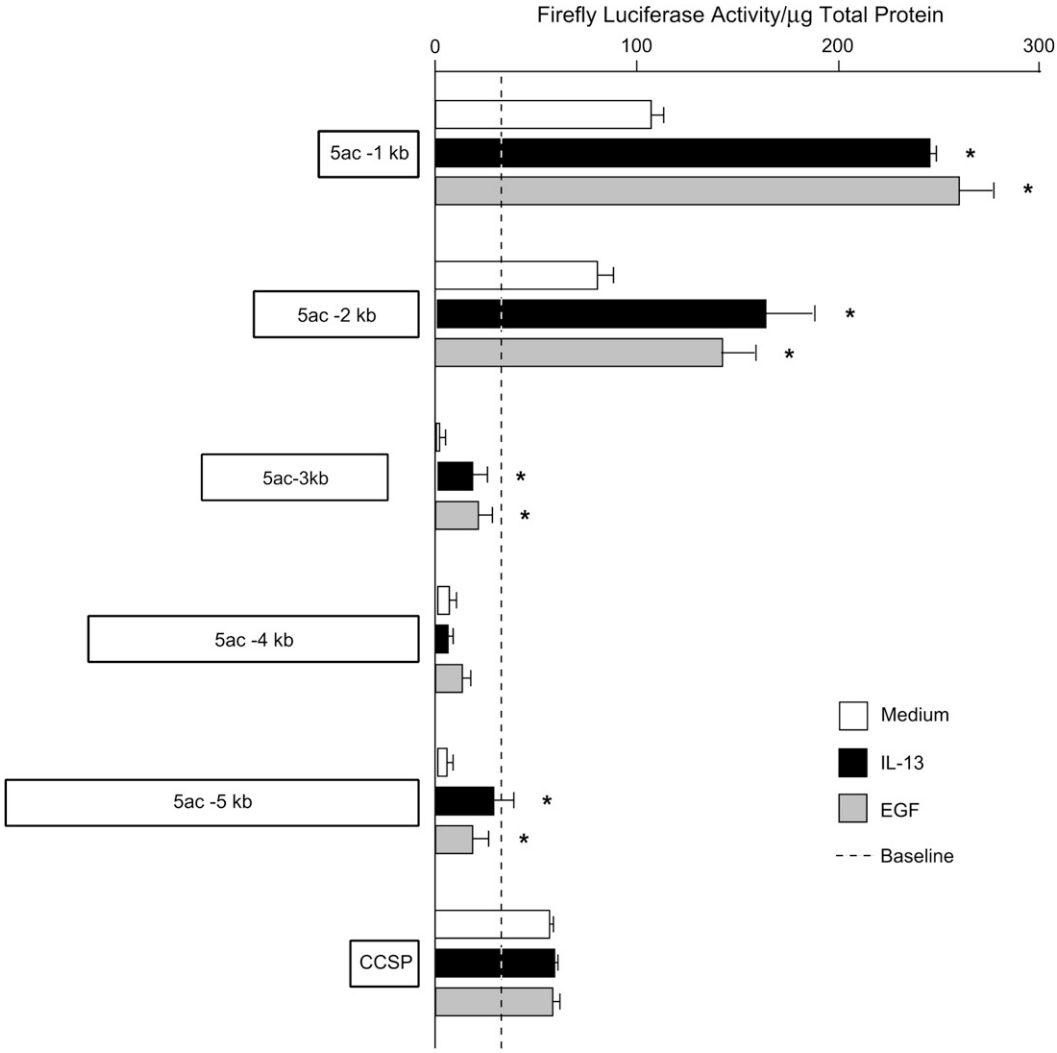

Figure 10. Activation of the Muc5ac promoter is cytokine inducible. Muc5ac promoter–luciferase constructs (1–5 kb) were transfected into mtCC1–2s and incubated overnight in serum-supplemented medium. Cells were serum starved for 6 h, followed by overnight incubation with SFM alone (*open bars*), 100 ng/ml recombinant mouse IL-13 (*solid bars*), or 25 ng/ml recombinant mouse EGF (*shaded bars*). The Muc5ac 5′ flanking region is differentially regulated in mtCC1–2s after IL-13 or EGF stimulation as compared with SFM (*open bars*). The 800-bp CCSP core promoter is unresponsive to IL-13 and EGF. *Dashed line* is luciferase activity in cells transfected with empty pGL3 vector. Data are presented as means ± SE in triplicate samples in a representative of six experiments. *Significant difference from medium alone.

that Muc5b functions as the chief homeostatic gel-forming mucin in mouse lungs, while Muc5ac functions as a pathophysiologic gel-forming mucin during disrupted homeostasis. Establishing the functional importance of these will depend on the generation and analysis of mice that constitutively express or are conditionally deficient in these mucin genes singly and in combination.

During allergic airway inflammation, the entire lung is exposed to IL-13. However, the responses of individual cell types vary greatly. For example, IL-13 is capable of directly acting on smooth muscle to modulate contractile responsiveness (42), but it clearly does not induce mucous metaplasia in airway smooth muscle or in other mesenchymal cells. Instead, the appearance of the mucous phenotype during IL-13–driven inflammation is restricted to secretory epithelial cells (5, 43). *In vitro*, the differential responsiveness of human epithelial cells, fibroblasts, and airway smooth muscle cells in primary cultures shows that many genes are differentially regulated by IL-13 in a tissue-specific manner (44). In addition to the differences observed between epithelial and mesenchymal responses, there are also differences observed between airway epithelial cell responses to redundant inflammatory signals such that ciliated and nonciliated epithelial cells demonstrate high specificity for several genes *in vivo*. For example, in mice, ciliated cell–specific genes encode TFs, such as Foxj1, and structural proteins, such as β-tubulin IV (45), while nonciliated cell specific genes encode secretory products, such as CCSP and Muc5ac, and components of the regulated exocytic machinery, such as Rab3D and Rab27a (5, 46). *In vivo*, there is differential regulation of mucin expression even within the Clara cell population of mice, since Muc5ac expression and histochemically detectable mucin granules are restricted to the bronchial airway Clara cell subset (Figure 3 and Ref. 5). One level of control of tissue-/cell-specific gene expression could be mediated by regulation of promoter and enhancer domains in the 5′ flanking regions of tissue-/cell-specific genes. However, in contrast to the high level of cross-species conservation within most protein-coding genomic DNA sequences, there is much less cross-species conservation within noncoding regions. The exceptions to this rule are found in genomic regions that contain functional regulatory elements that impart phylogenetically selective advantages. For example, an ∼ 400-bp conserved noncoding sequence (CNS-1) present in the IL-4/IL-13 intergene region regulates the polarization of CD4+ T cells (47), apparently by regulating the association of CNS-1 with modified histones during immune activation (48). In a preliminary attempt to gain insight into the mechanisms that control Muc5ac gene expression, we analyzed the 5′ noncoding regions of all sequenced mammalian MUC5AC orthologs. Our analysis revealed conservation within the first 5 kb of the human and mouse genes, with the highest conservation occurring in the *cis* region closest to the translation start site, where multiple TF recognition motifs reside. This region contains

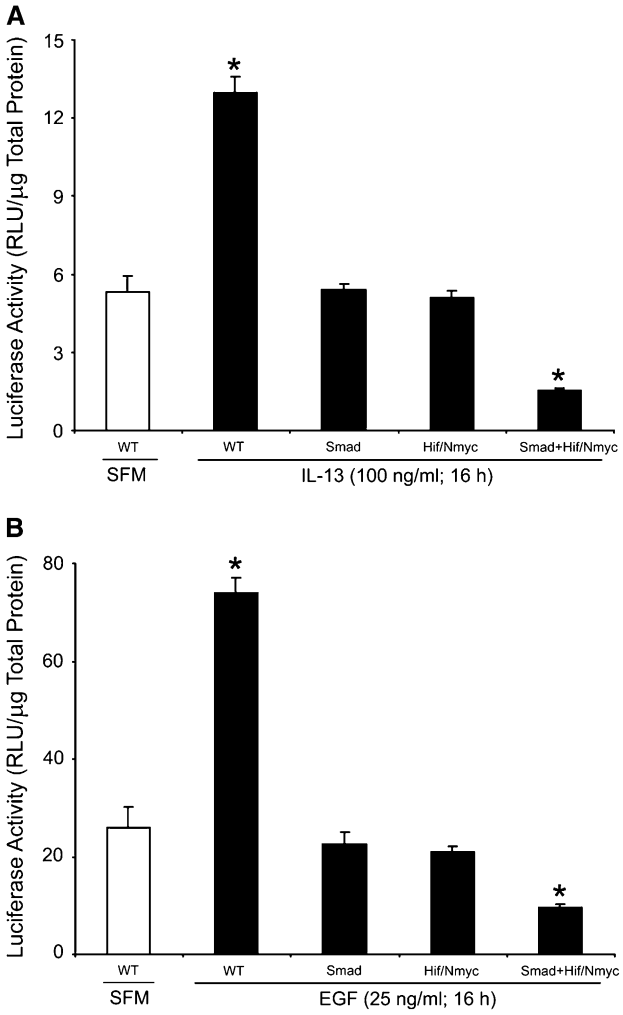

Figure 11. Cytokine inducible Muc5ac promoter activity is mediated by *cis* SMAD4 and HIF-1/Nmyc recognition motifs. Cultures of mtCC1–2s were transfected with 1 μg of wild-type and the SMAD4 and HIF-1/Nmyc mutant −1 kb Muc5ac firefly luciferase constructs used in Figure 9 and incubated in the presence of 10% FBS overnight. The following day, cells were serum starved for 6 h and were incubated overnight in SFM alone (*open bars*), SFM supplemented with 100 ng/ml recombinant mouse IL-13 (*solid bars* in *A*), or SFM supplemented with 25 ng/ml recombinant mouse EGF (*solid bars* in *B*). Eighteen hours later, luciferase and BCA assays were performed. In cells transfected with the wild-type promoter IL-13 and EGF, both increase Muc5ac promoter activity compared with unstimulated cells. In cells transfected with the −1 kb promoter harboring mutant HIF or SMAD4 motifs, singly and in combination, IL-13 and EGF both fail to induce promoter activity. Data are presented as luciferase activity normalized to total protein within each well. Values are means ± SE of results from three separate transfection experiments performed in sextuplicate. *Significant difference from wild-type promoter-transfected cells cultured in SFM.

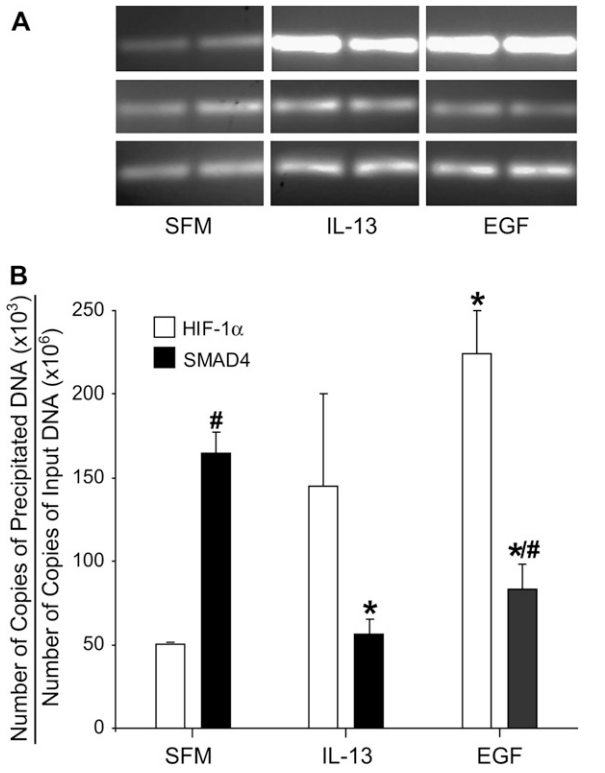

Figure 12. HIF-1α and SMAD4 bind to the Muc5ac promoter in mouse transformed Clara cells. Cells were cultured in the presence of 10% FBS until 75–90% confluent. Cells were then serum-starved for 6 h and were incubated overnight in SFM alone, SFM supplemented with 100 ng/ml recombinant mouse IL-13, or SFM supplemented with 25 ng/ml recombinant mouse EGF. Eighteen hours later, cells were fixed and lysed for chromatin immunoprecipitation (ChIP) using HIF-1α and SMAD4 Abs. (*A*) Nonquantitative PCR analysis of precipitated and input DNA using Muc5ac promoter–specific primers that flank the SMAD4 and HIF-1α TF motifs (sense primer, −144 to −125 bp ; antisense primer +20 to +1; *see* Figure 4) demonstrates binding of HIF-1α and SMAD4 to the Muc5ac promoter at baseline and after cytokine stimulation. (*B*) Quantitative PCR analysis of precipitated DNA demonstrates that HIF-1α and SMAD4 both bind to the Muc5ac promoter at baseline, and SMAD4 binds ∼ 3 times more often. HIF-1α binding to the Muc5ac promoter increases in cytokine stimulated cells, but SMAD4 binding decreases. Assessment of DNA precipitated with control IgG demonstrated ∼ 10,000 to > 100,000-fold lower values than any of the values generated from PCR of DNA precipitated by SMAD4 and HIF-1α Abs. Template DNA was diluted 10-fold for PCR analysis of input in *A*. Values in *B* are means ± SE of results normalized to input from three separate ChIP experiments analyzed in triplicate. *Significant difference in HIF-1α and SMAD4 association with the Muc5ac promoter between cytokine stimulated cells and cells cultured in SFM. #Significant difference between SMAD4 and HIF-1α results in cells cultured under identical conditions.

a functional promoter in the −1/−2 kb region that drives reporter gene expression strongly in mtCC1–2s.

The Muc5ac 5′ flanking region also contains a strong repressor element in the −2/−3 kb domain. Thus, one mechanism for controlling the tight regulation of Muc5ac expression in Clara cells may be mediated through the −2/−3 kb domain. To confirm whether this is a broad nonspecific gene silencing effect or a more selective or gene inhibitory event, we tested whether the −2/−3 kb domain could affect the expression of broad or cell-specific promoter-driven reporters. When the −2/−3 kb domain is fused to the constitutively active CMV promoter, the −2/−3 kb repressor has no effect on luciferase activity, indicating that it does not induce ubiquitous gene silencing. However, when fused to the CCSP promoter, the −2/−3kb domain abolishes luciferase activity (*see* Figure 8). It is thus conceivable that the −2/−3 kb repressor continuously blocks Muc5ac gene activation in distal airway Clara cells even in the presence of up-regulated mucin-inducing stimuli by acting on one or more identical or

related TF(s) present in the core promoters of both Muc5ac and CCSP (Figure 10), but this assertion needs to be tested *in vivo*. Other genes also show heterogeneous expression in secretory cell subsets and (like Muc5ac) show inducible regulation *in vivo*. These include the A_3 adenosine receptor (51, 52), Clca's (49, 50), and chitinases (53, 54). Analysis of the signal transduction pathways that lead to their induction and the TFs that up-regulate these will help to establish a hierarchy of components involved in a metaplastic network that controls goblet cell differentiation in the lungs.

Development of the mucous metaplastic phenotype in the lungs is a parenchymal response that occurs in response to many different inflammatory stimuli. To date, the best characterized inflammatory pathway leading to mucous metaplasia in mice is the Th2 lymphocyte–mediated allergen challenge model. Our initial studies demonstrated that the Th2 cytokine IL-13 activate Muc5ac gene transcription in mtCC1–2s, suggesting that an IL-13–responsive element is present in this region (5). However, sequence analysis of the Muc5ac 5′ flanking region shows no consensus motif for STAT6 (5′-TTCN$_4$GAA-3′), the IL-4 receptor α signal transduction molecule that is crucial for antigen and IL-13–induced goblet cell metaplasia *in vivo* (55, 56). Furthermore, the lack of any evolutionarily conserved STAT6 consensus sequences within the entire 5′ intergene regions of the mammalian MUC5AC orthologs suggests that a different gene regulatory mechanism is used. Recently, in differentiated airway epithelial cell cultures, IL-13 was shown to induce MUC5AC expression via a mechanism requiring a secondary TGF-β_2–mediated signal (57). These studies demonstrated that the "direct" effects of IL-13 on Muc5ac expression within the airway epithelium are mediated indirectly via the initiation of para-/autocrine activation of TGF-β_2/SMAD signal transduction pathways through a STAT6-dependent pathway. In support of this, both IL-4 and IL-13 both strongly up-regulate TGF-β_2 production in cultured airway epithelial cells (58). The core promoter of mouse Muc5ac contains a SMAD4 recognition site that is conserved across mammalian species (*see* Figures 4 and 5), and has been previously shown to be active in gain-of-function transfection studies (59). Furthermore, SMAD4 associates with this DNA region in mtCC1–2s, and mutation of this site significantly impairs reporter gene activity (Figures 9 and 11). Surprisingly, though, SMAD4 binding to this region of the Muc5ac promoter in mtCC1–2s decreases in response to IL-13 and EGF (Figure 12). These data suggest that SMAD4 constitutively binds the Muc5ac promoter, where it awaits interaction with other activating TFs that displace it. Future experiments testing the binding of activated forms of the TGF-β–responsive regulatory SMADs, phospho-SMAD2 and -3, to the Muc5ac promoter will clarify this.

Our studies also revealed the presence of a conserved consensus motif for the basic helix-loop-helix TFs HIF-1 and Nmyc that is adjacent to the SMAD4 site described above. Mutation of this site significantly impairs reporter gene activity, and mutation of this in combination with the adjacent SMAD4 site virtually abolishes reporter gene activity (Figure 9). Nmyc can function both as a transcriptional activator and as a repressor, but little Nmyc is expressed in the lungs at baseline in adult mice (60). However, in developing mouse embryos Nmyc is expressed in distal airways during the pseudoglandular and canalicular stages, where it critically regulates distal airway formation and differentiation of the bronchiolar airway epithelium (60). *Drosophila* homologs of the mammalian HIF-1 complex, typically comprised of HIF-1α and β, are expressed in the tracheal tube system, where they regulate tube formation (61; for reviews, *see* Refs. 62, 63). In vertebrates, the classical pathway of HIF-1 regulation uses the Krebs cycle metabolite 2-oxoglutarate (also called α-ketoglutarate) as a substrate for prolyl hydroxylase domain (PHD) and asparaginyl hydroxylase (also called FIH1 [factor inhibiting HIF-1]) enzymes to regulate HIF-1α stability and transactivation, respectively. These enzymes thus function as oxygen sensors by directly using products of aerobic metabolism to control the activation of hypoxia-responsive genes, which include vascular endothelial growth factor and erythropoietin, cytokines that regulate oxygen uptake and delivery. HIF-1 is increased in the lungs of experimental animals *in vivo* after hypoxic conditioning and challenge (64). The airway surface mucus layer of patients with CF shows steep oxygen gradients, such that the deepest region that is directly juxtaposed to the epithelial surface is nearly anoxic, creating conditions that favor the increased *Pseudomonas aeruginosa* alginate production and virulence (65). Thus, local hypoxic conditions are generated endogenously, and these may relay stressed cell signaling events via changes in the expression of HIF-1–responsive genes.

Under some conditions of cellular stress, HIF-1 may also be functional during normoxia. Mechanisms for this that have been demonstrated thus far include: (*1*) the induction of HIF-1α mRNA and protein production to such a degree that the classical oxygen-dependent degradative pathway is overwhelmed; (*2*) modification of HIF-1α by phosphorylation to prevent binding by PHDs or FIH1; or (*3*) phosphorylation of PHDs or FIH1 such that these fail to hydroxylate HIF-1α. Epidermal growth factor receptor (EGFR) signaling is prominent during cellular stress, and it induces HIF-1α mRNA synthesis. Downstream effectors of EGFR activation include p38 mitogen-activated protein kinase (MAPK), extracellular signal–regulated kinases (ERKs), and phosphoinositide-3-kinase (PI3K). PI3K, ERK, and p38 activation after cytokine stimulation increase HIF pathway activation under normoxic conditions by inducing high HIF-1α mRNA levels (66–69). ERK-mediated phosphorylation of HIF-1α inhibits FIH-mediated hydroxylation and subsequently to increased (disinhibited) HIF-1/CBP/p300 interaction (70–75). TGF-β increases HIF-1α protein stabilization through SMAD-dependent down-regulation of PHD2 in cultured epithelial cells and fibroblasts during normoxia (76). Importantly, these growth factor–mediated pathways function differently from the classical pathway, which can be activated ubiquitously, by introducing a layer of cell specificity via regulation of ligand and receptor expression (77). EGFR expression is up-regulated in the airway epithelium of humans with asthma (78–80), CF (81), and COPD (82, 83), and EGFR activation is critical for the induction of Muc5ac and mucous metaplasia in animal models and the up-regulation of MUC5AC in human airway epithelial cells in response allergens, viruses, neutrophils, and cigarette smoke (7, 84–88). While a great deal of effort has been placed on understanding the mechanisms of increased EGFR activation (e.g., by TNF-α–converting enzyme and matrix metalloproteinases) in response to extracellular oxidants and proteases (reviewed in Ref. 89), the intracellular mechanisms that relay EGFR activation and signal transduction at *cis* sites in the MUC5AC gene remain largely unexplained. In the present studies, EGF potently stimulates Muc5ac mRNA production in mtCC1–2s. Furthermore, EGF stimulates HIF-1α binding to the Muc5ac promoter, and it activates Muc5ac promoter activation via a *cis* HIF-1 TF motif. Thus, in the lungs, EGFR-dependent induction of HIF-1 may be an important mechanism for up-regulation of MUC5AC production and mucous metaplasia.

The findings presented here suggest that cell injury/damage response signals operate in a coordinated manner to regulate Muc5ac production and mucous metaplasia through multiple physical and genetic interactions. SMADs are known to interact with a large number of sequence-specific TFs in *Drosophila*, *Caenorhabditis elegans*, and vertebrates. HIF-1 interacts with

TGF-β signaling both physically and genetically via protein–protein interaction between HIF-1α and SMAD3 to mediate cooperative up-regulation of the vascular endothelial growth factor gene promoter (90) and via autocrine activation of the TGF- β_2 promoter through HIF-1α and SMAD3 binding (91). The close proximity and use of Smad4 and Hif-1 TF binding sites in the Muc5ac promoter suggests that these cellular stress and injury response signals interact to mediate Muc5ac production after inflammatory cell–mediated tissue damage *in vivo*. The human and mouse TGF-β_2 genes do not have conserved STAT6 consensus motifs within 20 kb upstream of their translational start sites (C. M. Evans, unpublished observation). Thus, like Muc5ac expression, it is also unlikely that TGF-β_2 expression is directly affected by STAT6 signaling. In contrast to Muc5ac and TGF-β_2, however, the promoter regions of the sequenced mammalian HIF-1α genes contain conserved canonical STAT6-binding motifs at −1067/−1058 (human) −1066/−1057 (chimpanzee), −1207/−1198 and −672/−663 (dog), −646/−637 (rat), and −658/−649 (mouse) upstream of their respective translational start sites (Figure E3). A model in which IL-13 regulates the differential expression of HIF-1α in the airway epithelium and thereby mediates the efficiency and localization of SMAD-mediated transcriptional activation within these anatomical sites under conditions of allergic lung inflammation is thus plausible. Further work *in vivo* using gain-/loss-of-function mutant and transgenic reporter animals will be critical for gaining a better understanding of the importance and hierarchy of these signals in Muc5ac expression.

Previous studies of the human MUC5AC promoter focused on direct relationships between pro- and anti-inflammatory mediators acting upon *cis* elements within the MUC5AC promoter. Two of these studies used *in vitro* reporter assays to identify potential roles for NF-κB and glucocorticoid-responsive elements (GREs) in activation and repression of the MUC5AC promoter (92, 93). Biochemical evidence using extracts from MUC5AC-expressing A549 adenocarcinoma cells suggests at least one GRE binds to the MUC5AC promoter in *cis*, but functional studies confirming the role of this site using mutant luciferase reporter constructs are lacking (93). Conversely, the findings implicating NF-κB as a *cis* acting factor were performed using transfected mutant reporter constructs; however, without biochemical analyses to confirm the binding of NF-κB subunits to the MUC5AC promoter, the functional importance of these findings remains questionable (92). Alignment of the 5′ flanking regions of MUC5AC orthologs does not reveal any well-conserved NF-κB sites or GREs (Figure E3). In agreement with this, previous investigations have demonstrated that epithelial expression of NF-κB is not required for the induction of Muc5ac expression and goblet cell metaplasia under conditions of allergic inflammation *in vivo*, since goblet cell metaplasia increases in NF-κB–deficient p50−/− mice receiving antigen-specific Th2 cells by adoptive transfer and subsequently exposed to antigen (94). Likewise, dexamethasone pretreatment only modestly decreases histochemically detectable goblet cell metaplasia in antigen challenged mice *in vivo* (95, 96). Thus, while these sites could have functional roles in regulating the human MUC5AC promoter, they are not suitable for future studies of Muc5ac promoter regulation in mice under allergic inflammatory conditions *in vivo*.

The model proposed here, of indirect Muc5ac regulation in response to inflammation via damage response signals, is a departure from the commonly held view that inflammatory signals directly mediate the bulk of MUC5AC promoter activation, but it is supported by previous findings *in vivo*. For example, in antigen-challenged mice, the induction and maximal levels of mucous metaplasia occur as inflammatory cell and cytokine levels wane, suggesting that some component(s) of these initiates the activation of secondary signals that mediate a temporally dissociated parenchymal response to inflammatory challenge (97). In addition, β-catenin, which is ordinarily activated during lung development (98) or in response to disruption of intercellular adherens junction contacts after cellular injury (99), induces spontaneous mucous metaplasia when overexpressed as a constitutively active transgene (100). A role for β-catenin signaling in the control of Muc5ac production is suggested here by our finding that Muc5ac promoter activity is significantly impaired by mutation of the *cis* recognition motif for Lef-1 (*see* Figure 8), a TF that transmits β-catenin signals in the nucleus (101, 102) and also cooperates with SMAD4 (103) to enhance gene transcription. Thus, signals released by epithelial damage, following exposure to inflammatory cells or exogenous stimuli, stimulate the expression of Muc5ac and the development of mucous metaplasia. Muc5ac expression and mucous metaplasia are phenotypic markers of lung inflammation induced by a wide variety of stimuli, including allergic, chemical, viral, and fungal challenges, that evoke highly disparate inflammatory signal transduction pathways. The use of these intracellular defense mechanisms to induce the mucous phenotype may be important for producing a redundant effector response to multiple divergent inflammatory signal transduction pathways.

In summary, the current study indicates that up-regulated Muc5ac expression is the central event in goblet cell metaplasia in antigen-challenged mice. This is an important finding, since mucus hypersecretion is associated with the development and progression of multiple lung disease processes. Therefore, blockade of Muc5ac expression is an ideal goal for reducing the pathological effects associated with airway mucus hypersecretion in mice. This approach would also be suitable in the airways of humans with asthma and COPD, where airflow obstruction and mucus plugging are most prominent in small airways (104, 105) where MUC5AC is the most abundant gel-forming mucin expressed by surface epithelial cells (39, 40). Muc5ac expression is tightly regulated such that its expression is temporally induced by cytokines specifically within secretory cells in the bronchial conducting airways. This regulatory process is mediated by a complex interaction of activator and repressor sites present within the 5′ flanking region that mediate Muc5ac gene expression in the airways in response to tissue stress/damage signals, such as TGF-β_2/SMAD, EGFR, and HIF-1, elicited during airway inflammation. Future studies testing the functional roles of conserved transcriptional regulatory networks *in vivo* will hopefully lead to the identification of novel targets for therapeutic interventions.

Conflict of Interest Statement: B.F.D. received $1,000 and 2,500 shares of common stock valued at approximately $1,000 for serving on the advisory board of BioMarck Pharmaceuticals in 2005, and his laboratory received a $65,000 contract from BioMarck for work with one of their compounds. None of the other authors has a financial relationship with a commercial entity that has an interest in the subject of this manuscript.

Acknowledgments: The authors thank Dr. Steve Georas and Dr. C. William Davis for helpful discussions. They also thank Blaga Iankova and Cecilia Clement for their technical assistance.

References

1. Wanner A, Salathe M, O'Riordan TG. Mucociliary clearance in the airways. *Am J Respir Crit Care Med* 1996;154:1868–1902.
2. Evans CM, Agrawal A, Dickey BF. Strategies to reduce excessive mucus secretion in airway inflammation. Eissa T, Huston D, editors. Therapeutic targets of airway inflammation. New York: Marcel Dekker; 2002.
3. Williams OW, Sharafkhaneh A, Kim V, Dickey BF, Evans CM. Airway mucus: from production to secretion. *Am J Respir Cell Mol Biol* 2006; 34:527–536.

4. Boers JE, Ambergen AW, Thunnissen FB. Number and proliferation of clara cells in normal human airway epithelium. *Am J Respir Crit Care Med* 1999;159:1585–1591.
5. Evans CM, Williams OW, Tuvim MJ, Nigam R, Mixides GP, Blackburn MR, DeMayo FJ, Burns AR, Smith C, Reynolds SD, *et al.* Mucin is produced by clara cells in the proximal airways of antigen-challenged mice. *Am J Respir Cell Mol Biol* 2004;31:382–394.
6. Wills-Karp M, Luyimbazi J, Xu X, Schofield B, Neben TY, Karp CL, Donaldson DD. Interleukin-13: central mediator of allergic asthma. *Science* 1998;282:2258–2261.
7. Takeyama K, Dabbagh K, Lee HM, Agusti C, Lausier JA, Ueki IF, Grattan KM, Nadel JA. Epidermal growth factor system regulates mucin production in airways. *Proc Natl Acad Sci USA* 1999;96:3081–3086.
8. Hollingsworth MA, Swanson BJ. Mucins in cancer: protection and control of the cell surface. *Nat Rev Cancer* 2004;4:45–60.
9. Stonebraker JR, Wagner D, Lefensty RW, Burns K, Gendler SJ, Bergelson JM, Boucher RC, O'Neal WK, Pickles RJ. Glycocalyx restricts adenoviral vector access to apical receptors expressed on respiratory epithelium in vitro and in vivo: role for tethered mucins as barriers to lumenal infection. *J Virol* 2004;78:13755–13768.
10. Thornton DJ, Sheehan JK. From mucins to mucus: toward a more coherent understanding of this essential barrier. *Proc Am Thorac Soc* 2004;1:54–61.
11. Escande F, Porchet N, Bernigaud A, Petitprez D, Aubert JP, Buisine MP. The mouse secreted gel-forming mucin gene cluster. *Biochim Biophys Acta* 2004;1676:240–250.
12. Chen Y, Zhao YH, Kalaslavadi TB, Hamati E, Nehrke K, Le AD, Ann DK, Wu R. Genome-wide search and identification of a novel gel-forming mucin MUC19/Muc19 in glandular tissues. *Am J Respir Cell Mol Biol* 2004;30:155–165.
13. Culp DJ, Latchney LR, Fallon MA, Denny PA, Denny PC, Couwenhoven RI, Chuang, S. The gene encoding mouse Muc19: CDNA, genomic organization and relationship to Smgc. *Physiol Genomics* 2004;19: 303–318.
14. Davies JR, Herrmann A, Russell W, Svitacheva N, Wickstrom C, Carlstedt I. Respiratory tract mucins: structure and expression patterns.*Novartis Found Symp* 2002;248:76–88.
15. Dohrman A, Miyata S, Gallup M, Li JD, Chapelin C, Coste A, Escudier E, Nadel J, Basbaum C. Mucin gene (MUC 2 and MUC 5AC) upregulation by gram-positive and gram-negative bacteria. *Biochim Biophys Acta* 1998;1406:251–259.
16. Chen Y, Zhao YH, Di YP, Wu R. Characterization of human mucin 5b gene expression in airway epithelium and the genomic clone of the amino-terminal and 5′-flanking region. *Am J Respir Cell Mol Biol* 2001;25:542–553.
17. Zudhi Alimam M, Piazza FM, Selby DM, Letwin N, Huang L, Rose MC. Muc-5/5ac mucin messenger RNA and protein expression is a marker of goblet cell metaplasia in murine airways. *Am J Respir Cell Mol Biol* 2000;22:253–260.
18. Reid CJ, Gould S, Harris A. Developmental expression of mucin genes in the human respiratory tract. *Am J Respir Cell Mol Biol* 1997;17: 592–598.
19. Bernacki SH, Nelson AL, Abdullah L, Sheehan JK, Harris A, Davis CW, Randell SH. Mucin gene expression during differentiation of human airway epithelia *in vitro*: muc4 and muc5b are strongly induced. *Am J Respir Cell Mol Biol* 1999;20:595–604.
20. Jono H, Shuto T, Xu H, Kai H, Lim DJ, Gum JR, Jr, Kim YS, Yamaoka S, Feng XH, Li JD. Transforming growth factor-beta-Smad signaling pathway cooperates with NF-kappa B to mediate nontypeable *Haemophilus influenzae*-induced MUC2 mucin transcription. *J Biol Chem* 2002;277:45547–45557.
21. Li JD, Dohrman AF, Gallup M, Miyata S, Gum JR, Kim YS, Nadel JA, Prince A, Basbaum CB. Transcriptional activation of mucin by *Pseudomonas aeruginosa* lipopolysaccharide in the pathogenesis of cystic fibrosis lung disease. *Proc Natl Acad Sci USA* 1997;94:967–972.
22. Shahzeidi S, Aujla PK, Nickola TJ, Chen Y, Alimam MZ, Rose MC. Temporal analysis of goblet cells and mucin gene expression in murine models of allergic asthma. *Exp Lung Res* 2003;29:549–565.
23. Magdaleno SM, Wang G, Jackson KJ, Ray MK, Welty S, Costa RH, DeMayo FJ. Interferon-gamma regulation of clara cell gene expression: *in vivo* and *in vitro*. *Am J Physiol* 1997;272:L1142–L1151.
24. Albrecht U, Eichele G, Helms J, Lu H. Visualization of gene expression patterns by in situ hybridization. Daston G. Molecular and cellular methods in developmental toxicology. Boca Raton, FL: CRC Press, Inc.; 1997. pp. 23–48.
25. Li D, Gallup M, Fan N, Szymkowski DE, Basbaum CB. Cloning of the amino-terminal and 5′-flanking region of the human MUC5AC mucingene and transcriptional up-regulation by bacterial exoproducts. *J Biol Chem* 1998;273:6812–6820.
26. Quandt K, Frech K, Karas H, Wingender E, Werner T. MatInd and MatInspector: new fast and versatile tools for detection of consensus matches in nucleotide sequence data. *Nucleic Acids Res* 1995;23:4878–4884.
27. Ovcharenko I, Loots GG, Hardison RC, Miller W, Stubbs L. ZPicture: dynamic alignment and visualization tool for analyzing conservation profiles. *Genome Res* 2004;14:472–477.
28. Jegga AG, Sherwood SP, Carman JW, Pinski AT, Phillips JL, Pestian JP, Aronow BJ. Detection and visualization of compositionally similar cis-regulatory element clusters in orthologous and coordinately controlled genes. *Genome Res* 2002;12:1408–1417.
29. Schwartz S, Zhang Z, Frazer KA, Smit A, Riemer C, Bouck J, Gibbs R, Hardison R, Miller W. PipMaker–a web server for aligning two genomic DNA sequences. *Genome Res* 2000;10:577–586.
30. Loots GG, Ovcharenko I. RVISTA 2.0: evolutionary analysis of transcription factor binding sites. *Nucleic Acids Res* 7–1–2004;32:W217–W221.
31. Ramsay PL, Luo Z, Magdaleno SM, Whitbourne SK, Cao X, Park MS, Welty SE, Yu-Lee LY, DeMayo FJ. Transcriptional regulation of CCSP by interferon-gamma in vitro and in vivo. *Am J Physiol Lung Cell Mol Physiol* 2003;284:L108–L118.
32. Postigo AA, Depp JL, Taylor JJ, Kroll KL. Regulation of Smad signaling through a differential recruitment of coactivators and corepressors by ZEB proteins. *EMBO J* 2003;22:2453–2462.
33. Riese J, Yu X, Munnerlyn A, Eresh S, Hsu SC, Grosschedl R, Bienz M. LEF-1, a nuclear factor coordinating signaling inputs from wingless and decapentaplegic. *Cell* 1997;88:777–787.
34. Ning W, Li CJ, Kaminski N, Feghali-Bostwick CA, Alber SM, Di YP, Otterbein SL, Song R, Hayashi S, Zhou Z,*et al*. Comprehensive gene expression profiles reveal pathways related to the pathogenesis of chronic obstructive pulmonary disease. *Proc Natl Acad Sci USA* 2004;101:14895–14900.
35. Chen Y, Zhao YH, Wu R. *In silico* cloning of mouse Muc5b gene and upregulation of its expression in mouse asthma model. *Am J Respir Crit Care Med* 2001;164:1059–1066.
36. Fallon MA, Latchney LR, Hand AR, Johar A, Denny PA, Georgel PT, Denny PC, Culp DJ. The Sld mutation is specific for sublingual salivary mucous cells and disrupts apomucin gene expression. *Physiol Genomics* 2003;14:95–106.
37. Carlstedt I, Herrmann A, Karlsson H, Sheehan J, Fransson LA, Hansson GC. Characterization of two different glycosylated domains from the insoluble mucin complex of rat small intestine. *J Biol Chem* 1993; 268:18771–18781.
38. Velcich A, Yang W, Heyer J, Fragale A, Nicholas C, Viani S, Kucherlapati R, Lipkin M, Yang K, Augenlicht L. Colorectal cancer in mice genetically deficient in the mucin Muc2. *Science* 2002;295:1726–1729.
39. Ordonez CL, Khashayar R, Wong HH, Ferrando R, Wu R, Hyde DM, Hotchkiss JA, Zhang Y, Novikov A, Dolganov G, *et al.* Mild and moderate asthma is associated with airway goblet cell hyperplasia and abnormalities in mucin gene expression. *Am J Respir Crit Care Med* 2001;163:517–523.
40. Innes AL, Woodruff PG, Ferrando RE, Donnelly S, Dolganov GM, Lazarus SC, Fahy JV. Epithelial mucin stores are increased in the large airways of smokers with airflow obstruction. *Chest* 2006;130: 1102–1108.
41. Zhu Y, Davis CW. The Munc13–2 null mouse reveals clara cells as natural mucin secreting cells [abstract]. *Pediatr Pulmonol* 2006;29:257.
42. Laporte JC, Moore PE, Baraldo SIMO, Jouvin MH, Church TL, Schwartzman IN, Panettieri RA, Jr., Kinet JP, Shore SA. Direct effects of interleukin-13 on signaling pathways for physiological responses in cultured human airway smooth muscle cells. *Am J Respir Crit Care Med* 2001;164:141–148.
43. Kim S, Shim JJ, Burgel PR, Ueki IF, Dao-Pick T, Tam DC, Nadel JA. IL-13-induced clara cell secretory protein expression in airway epithelium: role of EGFR signaling pathway. *Am J Physiol Lung Cell Mol Physiol* 2002;283:L67–L75.
44. Lee JH, Kaminski N, Dolganov G, Grunig G, Koth L, Solomon C, Erle DJ, Sheppard D. Interleukin-13 induces dramatically different transcriptional programs in three human airway cell types. *Am J Respir Cell Mol Biol* 2001;25:474–485.
45. Blatt EN, Yan XH, Wuerffel MK, Hamilos DL, Brody SL. Forkhead transcription factor HFH-4 expression is temporally related to ciliogenesis. *Am J Respir Cell Mol Biol* 1999;21:168–176.
46. Tolmachova T, Anders R, Stinchcombe J, Bossi G, Griffiths GM, Huxley C, Seabra MC. A general role for Rab27a in secretory cells. *Mol Biol Cell* 2004;15:332–344.

47. Mohrs M, Blankespoor CM, Wang ZE, Loots GG, Afzal V, Hadeiba H, Shinkai K, Rubin EM, Locksley RM. Deletion of a coordinate regulator of type 2 cytokine expression in mice. *Nat Immunol* 2001; 2:842–847.
48. Grogan JL, Wang ZE, Stanley S, Harmon B, Loots GG, Rubin EM, Locksley RM. Basal chromatin modification at the IL-4 gene in helper T cells. *J Immunol* 2003;171:6672–6679.
49. Patel AC, Morton JD, Kim EY, Alevy Y, Swanson S, Tucker J, Huang G, Agapov E, Phillips TE, Fuentes ME,*et al*. Genetic segregation of airway disease traits despite redundancy of calcium-activated chloride channel family members. *Physiol Genomics* 2006;25:502–513.
50. Nakanishi A, Morita S, Iwashita H, Sagiya Y, Ashida Y, Shirafuji H, Fujisawa Y, Nishimura O, Fujino M. Role of Gob-5 in mucus overproduction and airway hyperresponsiveness in asthma. *Proc Natl Acad Sci USA* 2001;98:5175–5180.
51. Blackburn MR, Lee CG, Young HWJ, Zhu Z, Chunn JiL, Kang MJ, Banerjee SK, Elias JA. Adenosine mediates IL-13-induced inflammation and remodeling in the lung and interacts in an IL-13-adenosine amplification pathway. *J Clin Invest* 2003;112:332–344.
52. Young HWJ, Molina JG, Dimina D, Zhong H, Jacobson M, Chan LN, Chan TS, Lee JJ, Blackburn MR. A3 adenosine receptor signaling contributes to airway inflammation and mucus production in adenosine deaminase-deficient mice. *J Immunol* 2004;173:1380–1389.
53. Homer RJ, Zhu Z, Cohn L, Lee CG, White WI, Chen S, Elias JA. Differential expression of chitinases identify subsets of murine airway epithelial cells in allergic inflammation. *Am J Physiol Lung Cell Mol Physiol* 2006;291:L502–L511.
54. Zhu Z, Zheng T, Homer RJ, Kim YK, Chen NY, Cohn L, Hamid Q, Elias JA. Acidic mammalian chitinase in asthmatic Th2 inflammation and IL-13 pathway activation. *Science* 2004;304:1678–1682.
55. Kuperman D, Schofield B, Wills-Karp M, Grusby MJ. Signal transducer and activator of transcription factor 6 (Stat6)-deficient mice are protected from antigen-induced airway hyperresponsiveness and mucus production. *J Exp Med* 1998;187:939–948.
56. Kuperman DA, Huang X, Koth LL, Chang GH, Dolganov GM, Zhu Z, Elias JA, Sheppard D, Erle DJ. Direct effects of interleukin-13 on epithelial cells cause airway hyperreactivity and mucus overproduction in asthma. *Nat Med* 2002;8:885–889.
57. Chu HW, Balzar S, Seedorf GJ, Westcott JY, Trudeau JB, Silkoff P, Wenzel SE. Transforming growth factor-beta2 induces bronchial epithelial mucin expression in asthma. *Am J Pathol* 2004;165:1097–1106.
58. Wen FQ, Kohyama T, Liu X, Zhu YK, Wang H, Kim HJ, Kobayashi T, Abe S, Spurzem JR, Rennard SI. Interleukin-4- and interleukin-13-enhanced transforming growth factor-beta2 production in cultured human bronchial epithelial cells is attenuated by interferon-gamma. *Am J Respir Cell Mol Biol* 2002;26:484–490.
59. Jonckheere N, van der Sluis M, Velghe A, Buisine MP, Sutmuller M, Ducourouble MP, Pigny P, Buller HA, Aubert JP, Einerhand AW, *et al*. Transcriptional activation of the murine muc5ac mucin gene in epithelial cancer cells by TGF-Beta/Smad4 signalling pathway is potentiated by Sp1. *Biochem J* 2004;377:797–808.
60. Okubo T, Knoepfler PS, Eisenman RN, Hogan BL. Nmyc plays an essential role during lung development as a dosage-sensitive regulator of progenitor cell proliferation and differentiation. *Development* 2005;132:1363–1374.
61. Jarecki J, Johnson E, Krasnow MA. Oxygen regulation of airway branching in Drosophila is mediated by branchless FGF. *Cell* 1999;99: 211–220.
62. Warburton D, Schwarz M, Tefft D, Flores-Delgado G, Anderson KD, Cardoso WV. The molecular basis of lung morphogenesis. *Mech Dev* 2000;92:55–81.
63. Ghabrial A, Luschnig S, Metzstein MM, Krasnow MA. Branching morphogenesis of the Drosophila tracheal system. *Ann Rev Cell Dev Biol* 2003;19:623–647.
64. Yu AY, Frid MG, Shimoda LA, Wiener CM, Stenmark K, Semenza GL. Temporal, Spatial, and Oxygen-Regulated Expression of Hypoxia-Inducible Factor-1 in the Lung. *Am J Physiol* 1998;275:L818–L826.
65. Worlitzsch D, Tarran R, Ulrich M, Schwab U, Cekici A, Meyer KC, Birrer P, Bellon G, Berger J, Weiss T, *et al.* Effects of reduced mucus oxygen concentration in airway Pseudomonas infections of cystic fibrosis patients. *J Clin Invest* 2002;109:317–325.
66. Fukuda R, Hirota K, Fan F, Jung YD, Ellis LM, Semenza GL. Insulin-like growth factor 1 induces hypoxia-inducible factor 1-mediated vascular endothelial growth factor expression, which is dependent on MAP kinase and phosphatidylinositol 3-kinase signaling in colon cancer cells. *J Biol Chem* 2002;277:38205–38211.
67. Laughner E, Taghavi P, Chiles K, Mahon PC, Semenza GL. HER2 (Neu) signaling increases the rate of hypoxia-inducible factor 1alpha (HIF-1alpha) synthesis: novel mechanism for HIF-1-mediated vascular endothelial growth factor expression. *Mol Cell Biol* 2001;21:3995–4004.
68. Zhong H, Chiles K, Feldser D, Laughner E, Hanrahan C, Georgescu MM, Simons JW, Semenza GL. Modulation of hypoxia-inducible factor 1alpha expression by the epidermal growth factor/phosphatidylinositol 3-kinase/PTEN/AKT/FRAP pathway in human prostate cancer cells: implications for tumor angiogenesis and therapeutics. *Cancer Res* 2000;60:1541–1545.
69. Zundel W, Schindler C, Haas-Kogan D, Koong A, Kaper F, Chen E, Gottschalk AR, Ryan HE, Johnson RS, Jefferson AB, *et al*. Loss of PTEN facilitates HIF-1-mediated gene expression. *Genes Dev* 2000; 14:391–396.
70. Gradin K, Takasaki C, Fujii-Kuriyama Y, Sogawa K. The transcriptional activation function of the HIF-like factor requires phosphorylation at a conserved threonine. *J Biol Chem* 2002;277:23508–23514.
71. Lancaster DE, McNeill LA, McDonough MA, Aplin RT, Hewitson KS, Pugh CW, Ratcliffe PJ, Schofield CJ. Disruption of dimerization and substrate phosphorylation inhibit factor inhibiting hypoxia-inducible factor (FIH) activity. *Biochem J* 2004;383:429–437.
72. Sang N, Stiehl DP, Bohensky J, Leshchinsky I, Srinivas V, Caro J. MAPK signaling up-regulates the activity of hypoxia-inducible factors by its effects on P300. *J Biol Chem* 2003;278:14013–14019.
73. Sang N, Fang J, Srinivas V, Leshchinsky I, Caro J. Carboxyl-terminal transactivation activity of hypoxia-inducible factor 1 alpha is governed by a von hippel-lindau protein-independent, hydroxylation-regulated association with P300/CBP. *Mol Cell Biol* 2002;22:2984–2992.
74. Richard DE, Berra E, Gothie E, Roux D, Pouyssegur J. P42/P44 mitogen-activated protein kinases phosphorylate hypoxia-inducible factor 1alpha (HIF-1alpha) and enhance the transcriptional activity of HIF-1. *J Biol Chem* 1999;274:32631–32637.
75. Sodhi A, Montaner S, Patel V, Zohar M, Bais C, Mesri EA, Gutkind JS. The Kaposi's sarcoma-associated herpes virus g protein-coupled receptor up-regulates vascular endothelial growth factor expression and secretion through mitogen-activated protein kinase and P38 pathways acting on hypoxia-inducible factor 1alpha. *Cancer Res* 2000;60: 4873–4880.
76. McMahon S, Charbonneau M, Grandmont S, Richard DE, Dubois CM. TGFbeta 1 induces HIF-1 stabilization through selective inhibition of PHD2 expression. *J Biol Chem* 2006;281:24171–24181.
77. Semenza GL. Targeting HIF-1 for cancer therapy. *Nat Rev Cancer* 2003; 3:721–732.
78. Takeyama K, Fahy JV, Nadel JA. Relationship of epidermal growth factor receptors to goblet cell production in human bronchi. *Am J Respir Crit Care Med* 2001;163:511–516.
79. Amishima M, Munakata M, Nasuhara Y, Sato A, Takahashi T, Homma Y, Kawakami Y. Expression of epidermal growth factor and epidermal growth factor receptor immunoreactivity in the asthmatic human airway. *Am J Respir Crit Care Med* 1998;157:1907–1912.
80. Polosa R, Puddicombe SM, Krishna MT, Tuck AB, Howarth PH, Holgate ST, Davies DE. Expression of C-ErbB receptors and ligands in the bronchial epithelium of asthmatic subjects. *J Allergy Clin Immunol* 2002;109:75–81.
81. Voynow JA, Fischer BM, Roberts BC, Proia AD. Basal-like cells constitute the proliferating cell population in cystic fibrosis airways. *Am J Respir Crit Care Med* 2005;172:1013–1018.
82. de Boer WI, Hau CM, van Schadewijk A, Stolk J, van Krieken JH, Hiemstra PS. Expression of epidermal growth factors and their receptors in the bronchial epithelium of subjects with chronic obstructive pulmonary disease. *Am J Clin Pathol* 2006;125:184–192.
83. O'Donnell RA, Richter A, Ward J, Angco G, Mehta A, Rousseau K, Swallow DM, Holgate ST, Djukanovic R, Davies DE, *et al.* Expression of ErbB receptors and mucins in the airways of long term current smokers. *Thorax* 2004;59:1032–1040.
84. Tyner JW, Kim EY, Ide K, Pelletier MR, Roswit WT, Morton JD, Battaile JT, Patel AC, Patterson GA, Castro M, *et al.* Blocking airway mucous cell metaplasia by inhibiting EGFR antiapoptosis and IL-13 transdifferentiation signals. *J Clin Invest* 2006;116:309–321.
85. Burgel PR, Lazarus SC, Tam DC, Ueki IF, Atabai K, Birch M, Nadel JA. Human eosinophils induce mucin production in airway epithelial cells via epidermal growth factor receptor activation. *J Immunol* 2001;167:5948–5954.
86. Shao MX, Nakanaga T, Nadel JA. Cigarette smoke induces MUC5AC mucin overproduction via tumor necrosis factor-alpha-converting

enzyme in human airway epithelial (NCI-H292) cells. *Am J Physiol Lung Cell Mol Physiol* 2004;287:L420–L427.
87. Shim JJ, Dabbagh I, Ueki I, Burgel P, Takeyama K, Tam DC, Nadel JA. IL-13 induces mucin production by stimulating epidermal growth factor receptors and by activating neutrophils. *Am J Physiol Lung Cell Mol Physiol* 2001;280:L134–L140.
88. Takeyama K, Jung B, Shim JJ, Burgel PR, Dao-Pick T, Ueki IF, Protin U, Kroschel P, Nadel JA. Activation of epidermal growth factor receptors is responsible for mucin synthesis induced by cigarette smoke. *Am J Physiol Lung Cell Mol Physiol* 2001;280:L165–L172.
89. Burgel PR, Nadel JA. Roles of epidermal growth factor receptor activation in epithelial cell repair and mucin production in airway epithelium. *Thorax* 2004;59:992–996.
90. Sanchez-Elsner T, Botella LM, Velasco B, Corbi A, Attisano L, Bernabeu C. Synergistic cooperation between hypoxia and transforming growth factor-beta pathways on human vascular endothelial growth factor gene expression. *J Biol Chem* 2001;276:38527–38535.
91. Zhang H, Akman HO, Smith EL, Zhao J, Murphy-Ullrich JE, Batuman OA. Cellular response to hypoxia involves signaling via Smad proteins. *Blood* 2003;101:2253–2260.
92. Chen R, Lim JH, Jono HI, Gu XX, Kim YS, Basbaum CB, Murphy TF, Li JD. Nontypeable Haemophilus influenzae lipoprotein P6 induces MUC5AC mucin transcription via TLR2–TAK1-dependent P38 MAPK-AP1 and IKKβ-IκBα-NF-κB signaling pathways. *Biochem Biophys Res Commun* 2004;324:1087–1094.
93. Chen Y, Nickola TrJ, DiFronzo NL, Colberg-Poley AM, Rose MC. Dexamethasone-mediated repression of MUC5AC gene expression in human lung epithelial cells. *Am J Respir Cell Mol Biol* 2005;34: 338–347.
94. Whittaker L, Niu N, Temann UA, Stoddard A, Flavell RA, Ray A, Homer RJ, Cohn L. Interleukin-13 mediates a fundamental pathway for airway epithelial mucus induced by CD4 T Cells and interleukin-9. *Am J Respir Cell Mol Biol* 2002;27:593–602.
95. Kumar RK, Herbert C, Thomas PS, Wollin L, Beume R, Yang M, Webb DC, Foster PS. Inhibition of inflammation and remodeling by roflumilast and dexamethasone in murine chronic asthma. *J Pharmacol Exp Ther* 2003;307:349–355.
96. Trifilieff A, Ahmed E, Bertrand C. Time course of inflammatory and remodeling events in a murine model of asthma: effect of steroid treatment. *Am J Physiol Lung Cell Mol Physiol* 2000;279:L1120–L1128.
97. Tomkinson A, Cieslewicz G, Duez C, Larson KA, Lee JJ, Gelfand EW. Temporal association between airway hyperresponsiveness and airway eosinophilia in ovalbumin-sensitized mice. *Am J Respir Crit Care Med* 2001;163:721–730.
98. Mucenski ML, Wert SE, Nation JM, Loudy DE, Huelsken J, Birchmeier W, Morrisey EE, Whitsett JA. Beta-catenin is required for specification of proximal/distal cell fate during lung morphogenesis. *J Biol Chem* 2003;278:40231–40238.
99. Park KS, Wells JM, Zorn AM, Wert SE, Laubach VE, Fernandez LG, Whitsett JA. Transdifferentiation of ciliated cells during repair of the respiratory epithelium. *Am J Respir Cell Mol Biol* 2006;34:151–157.
100. Mucenski ML, Nation JM, Thitoff AR, Besnard V, Xu Y, Wert SE, Harada N, Taketo MM, Stahlman MT, Whitsett JA. Beta-catenin regulates differentiation of respiratory epithelial cells in vivo. *Am J Physiol Lung Cell Mol Physiol* 2005;289:L971–L979.
101. Aoki M, Hecht A, Kruse U, Kemler R, Vogt PK. Nuclear endpoint of Wnt signaling: neoplastic transformation induced by transactivating lymphoid-enhancing factor 1. *Proc Natl Acad Sci USA* 1999;96:139–144.
102. Novak A, Hsu SC, Leung-Hagesteijn C, Radeva G, Papkoff J, Montesano R, Roskelley C, Grosschedl R, Dedhar S. Cell adhesion and the integrin-linked kinase regulate the LEF-1 and beta-catenin signaling pathways. *Proc Natl Acad Sci USA* 1998;95:4374–4379.
103. Lim SK, Hoffmann FM. Smad4 Cooperates with lymphoid enhancer-binding factor 1/T cell-specific factor to increase C-Myc expression in the absence of TGF-beta signaling. *Proc Natl Acad Sci USA* 2006; 103:18580–18585.
104. Kirkham S, Sheehan JK, Knight D, Richardson PS, Thornton DJ. Heterogeneity of airways mucus: variations in the amounts and glycoforms of the major oligomeric mucins MUC5AC and MUC5B. *Biochem J* 2002;361:537–546.
105. Caramori G, Di Gregorio C, Carlstedt I, Casolari P, Guzzinati I, Adcock IM, Barnes PJ, Ciaccia A, Cavallesco G, Chung KF, *et al.* Mucin expression in peripheral airways of patients with chronic obstructive pulmonary disease. *Histopathology* 2004;45:477–484.